TLR9-deficiency in B cells Promotes Immune Tolerance via IL-10 in a Type 1 Diabetes Mouse Model

Running title: TLR9-deficiency in B cells in NOD

Sha Sha[1,2], James A Pearson[2], Jian Peng[2], Youjia Hu[2], Juan Huang[2], Yanpeng Xing[2,3], Luyao Zhang[2,3], Ying Zhu[4], Hongyu Zhao[4], F. Susan Wong[5], Li Chen[1], and Li Wen[2]

[1]Department of Endocrinology, Qilu Hospital of Shandong University, Jinan, Shandong, China; Institute of Endocrine and Metabolic Diseases of Shandong University, Jinan, Shandong, China; Key Laboratory of Endocrine and Metabolic Diseases, Shandong Province medicine& health, Jinan, Shandong, China.

[2] Section of Endocrinology, School of Medicine, Yale University, New Haven, CT, 06519, USA;

[3]Department of Gastrointestinal Surgery, The First Hospital of Jilin University, Changchun, Jilin, China

[4]Department of Biostatistics, School of Public Health, Yale University, New Haven, CT, 06519, USA;

[5]Division of Infection and Immunity, School of Medicine, Cardiff University, Cardiff, UK

Correspondence to:

Li Wen

Section of Endocrinology

School of Medicine

Yale University

New Haven

Connecticut

USA

E-mail: li.wen@yale.edu

Telephone: 203.785.7186

Authorship note: JAP and JP contributed equally to the work.

Word count: 4307

Number of tables: 1

Number of figures: 6

Diabetes Publish Ahead of Print, published online November 5, 2020

Abstract

Toll-like receptor 9 (TLR9) is highly expressed in B cells and B cells are important in the pathogenesis of type 1 diabetes (T1D) development. However, the intrinsic effect of TLR9 in B cells on beta cell autoimmunity is not known. To fill this knowledge gap, we generated non-obese diabetic (NOD) mice with a B cell-specific deficiency of TLR9 ($TLR9^{fl/fl}$/CD19-Cre+ NOD). The B cell-specific deletion of TLR9 resulted in near complete protection from T1D development. Diabetes protection was accompanied by an increased proportion of IL-10-producing B cells. We also found that TLR9-deficient B cells were hyporesponsive to both innate and adaptive immune-stimuli. This suggested that TLR9 in B cells modulates T1D susceptibility in NOD mice by changing the frequency and function of IL-10-producing B cells. Molecular analysis revealed a network of TLR9 with MMPs, TIMP1 and CD40, all of which are inter-connected with IL-10. Our study has highlighted an important connection of an innate immune molecule in B cells to the immuno-pathogenesis of T1D. Thus, targeting the TLR9 pathway, specifically in B cells, may provide a novel therapeutic strategy for T1D treatment.

Introduction

Toll-like receptors (TLRs) are innate immune receptors that recognize molecular patterns of microbial pathogens. On binding to the appropriate ligands, TLRs activate signaling pathways that lead to production of proinflammatory cytokines [1, 2] and upregulation of co-stimulatory molecules [3, 4]. TLR9 has been shown to be expressed on a range of immune cells including B cells [5, 6], dendritic cells (DCs) [7, 8], monocytes/macrophages [9, 10], T cells [11], epithelial cells [12, 13] and endothelial cells [14]. TLR9 recognizes CG-rich DNA from pathogens and self-DNA, as well as short single-stranded synthetic DNA, CpG [15, 16]. TLR9 stimulation induces downstream signaling, leading to the induction of a range of cytokines and the promotion or suppression of cell survival [17, 18]. TLR9 plays an important role in systemic autoimmune diseases, such as systemic lupus erythematosus (SLE), in both humans and a mouse model of human SLE [19-21]. In the absence of TLR9, autoimmune disease was exacerbated in a mouse model of SLE [22, 23]. Interestingly, a TLR9-deficient Non-Obese Diabetic (NOD) mouse model of human type 1 diabetes (T1D) was protected from T1D development [24, 25]. This protection was partly mediated by impaired IFNα production by dendritic cells (DCs) from the TLR9-/- mouse [25] and by enhanced expression and regulatory function of CD73+ T cells, as well as by enhanced islet β-cell function [24, 26].

Expression of TLRs in B cells provides a cell-intrinsic mechanism for innate signals regulating adaptive immune responses [22, 27], and studies have suggested that TLR signaling plays vital roles in B cell development and activation [6, 28, 29]. Increasing evidence also suggests that B cell activation by TLR9 ligands is important for optimal antibody responses to microbial antigens and DNAs released from both physiological and pathological dying cells [6, 30]. To address the intrinsic role of TLR9 in the function of B cells in a spontaneous autoimmune diabetes model system, we generated the non-obese diabetic (NOD) mouse model with a B cell-specific deficiency of TLR9 ($TLR9^{fl/fl}$CD19-Cre+ NOD). We hypothesized that TLR9 in B cells modulates T1D development by regulating immune tolerance to islet β-cell autoimmunity. Our results showed that B cell-specific TLR9 deficiency led to striking protection from T1D development in NOD mice. Mechanistic studies suggested that TLR9 regulates the IL-10-producing B cells and that TLR9 deficiency in the B cells changes the proportion and function of

IL-10-producing B cells that contribute to diabetes protection. The molecular mechanism of TLR9 regulation of IL-10-producing B cells was mediated by down-regulation of matrix metalloproteinases (MMPs) and up-regulation of tissue inhibitors of metalloproteinases (TIMPs) gene expression in B cells, leading to protection from diabetes development.

Research Design and Methods

Mice

Mice used in the study were housed in specific pathogen-free conditions with a 12 h dark–light cycle at the Yale University animal facility. $TLR9^{fl/fl}$ C57BL/6 mouse breeders were kindly provided by Mark Shlomchik (University of Pittsburgh) and were back-crossed to our NOD/Caj genetic background for over 10 generations. CD19-Cre NOD breeders were purchased from the Jackson Laboratory (Bar Harbor, ME, USA) and bred with our NOD/Caj mice. $TLR9^{fl/fl}$ and CD19-Cre NOD mice were then inter-crossed to obtain B cell-specific TLR9-deficient ($TLR9^{fl/fl}$ CD19-Cre+) and control ($TLR9^{fl/fl}$/CD19-Cre-) NOD mice. The total body TLR9- deficient (TLR9-/-) NOD mice were generated as previously reported [24, 26]. The use of the animals in this study was approved by the Institutional Animal Care and Use Committee of Yale University.

Diabetes incidence monitoring

Diabetes development in $TLR9^{fl/fl}$/CD19-Cre+ NOD mice and $TLR9^{fl/fl}$/CD19-Cre- NOD mice were monitored weekly for diabetes development by testing for glycosuria with glucose strips (Bayer, NJ, USA) from 10 to 32 weeks of age. Diabetes was diagnosed by two consecutive positive glycosuria tests, 24 hours apart and confirmed with a blood glucose reading of 250 mg/dl (13.9mmol/L), using a FreeStyle glucose meter (Abbott, Chicago, IL, USA).

Monoclonal antibody staining, tetramer staining and flow cytometry

Mononuclear cells were harvested from spleen, pancreatic lymph nodes (PLN), mesenteric lymph nodes (MLN), Peyer's Patches (PP) and peritoneal cavity (PC). Cells ($2\text{-}5x10^6$) were first incubated with an Fc blocking antibody (CD16/32,15 minutes, 4°C) prior to staining with antibodies against CD19, B220, CD40, TCR-beta, CD5, CD1d, CD21, CD23 and a viability dye

(all from BioLegend) for 30 minutes at 4°C. For intracellular cytokine (ICC) staining, the cells ($5x10^6$) were stimulated with PMA (50ng/ml, Sigma) and Ionomycin (500ng/ml, Sigma) in the presence of 1µl/ml GolgiPlug™ (BD) for 4 hours. Post-stimulation, the cells were stained as described above. After washing, fixation (20 mins at room temperature, RT) and permeabilization (eBioscience™ Intracellular fixation and permeabilization buffer), the cells were then incubated with an Fc blocking antibody (15 minutes, 4°C), prior to staining with antibodies against cytokines. PE-conjugated IGRP-tetramer ($IGRP_{206-214}$, VYLKTNVFL, NIH Tetramer Core Facility) staining was carried out with pre-titrated IGRP-tetramer together with antibodies against TCR-Vβ8, CD8α, CD44, CD62L, isotype control as well as viability dye. All the samples were analyzed with BD LSRII flow cytometry.

Cell isolation and cell depletion

Splenic B cells were isolated using the EasySep™ Mouse B cell purification kit (STEMCELL Technologies), following the manufacturer's protocol. Splenic $CD4^+$ T cells were isolated by removing $CD8^+$ T cells and antigen presenting cells (APCs). The splenocytes were incubated with hybridoma supernatants containing mAbs to CD8 (TB105) and MHC-II (10.2.16) for 30mins, at 4°C. After washing with PBS, the cells were further incubated for 45mins on ice with magnetic beads conjugated with goat anti-mouse IgG and IgM (to remove B cells) or goat anti-rat IgG to remove CD8+ and MHC-II+ cells (all the beads were from QIAGEN). $CD4^+$ T cells were then separated using a magnetic plate. The purity was routinely 90-95%, as verified by flow cytometry. To deplete splenic Treg cells, we removed $CD4^+CD25^+$ T cells by EasySep™ Mouse Treg isolation kit (STEMCELL Technologies) and the unbound cells were the Treg-depleted splenocytes that were used for adoptive transfer.

Cell culture and transwell co-culture system

Purified B cells (10^5/well) were stimulated with anti-CD40, with or without anti-IgM or different TLR ligands, for 2 days, and the proliferative response was determined by ^{3}H-thymidine incorporation. In a co-culture system, purified B cells, co-cultured with purified T subsets from $TLR9^{fl/fl}$/CD19-Cre- NOD mice, were stimulated with anti-CD3 and anti-CD28. In a transwell co-culture system, purified B cells (10^5/well) from $TLR9^{fl/fl}$/CD19-Cre+ NOD mice or

TLR9$^{fl/fl}$/CD19-Cre- NOD mice were added to the insert chambers; purified T cells (10^5/well) from wild type NOD mice, together with T cell-depleted APCs, (10^5/well), were plated in the bottom chamber, in the presence of anti-CD3 and anti-CD28 (final concentration 1μg/ml). For the IL-10 blocking transwell culture, anti-IL-10 receptor mAb (1B1.3A) or control rat IgG was added into the culture (insert chamber). All the cultures were incubated for 2 days in triplicate. ^{3}H-thymidine was then added and cell culture supernatants were collected. Cells were incubated for a further 18 hours before harvesting. Proliferation was determined by ^{3}H-Thymidine incorporation using a beta-counter and presented as counts per minute (CPM).

ELISA

Different isotypes of serum immunoglobulins were assessed using direct ELISA (Southern Biotech) and the concentrations were determined by standard curve for each isotype (Southern Biotech). IL-10 content of the cell culture supernatants and in serum was determined using the Mouse IL-10 ELISA MAX™ Standard kit (BioLegend), based on the manufacturer's protocol provided.

Adoptive transfer

Purified splenic T cells (5×10^6) from diabetic NOD mice, together with sorted splenic B cells (5×10^6) from 6-7-week-old TLR9$^{fl/fl}$/CD19-Cre+ or TLR9$^{fl/fl}$/CD19-Cre- NOD mice, were injected (i.v.) into 5-6-week-old female *Rag-/-* NOD mice. Another set of adoptive transfer experiments was carried out by transferring Treg-depleted splenocytes (10×10^6) from 6-7-week-old TLR9$^{fl/fl}$/CD19-Cre+ or TLR9$^{fl/fl}$/CD19-Cre- NOD mice into 5-6-week-old female *Rag-/-* NOD mice. All the recipients were monitored weekly for glycosuria, and the experiments were terminated 12 to 14 weeks after the cell transfer, unless the mice developed diabetes, which was confirmed by blood glucose greater than 250 mg/dL (13.9 mmol/l).

Microarray hybridization and data analysis

Total RNA was extracted from sorted splenic B cells from TLR9$^{fl/fl}$/CD19-Cre+ or TLR9$^{fl/fl}$/CD19-Cre- NOD mice (7-8-week-old females) with RNeasy Mini kit (Qiagen). cRNA synthesis and whole genome Illumina microarray chip analysis were carried out at the Yale

Center for Genomic Analysis. Gene expression data was normalized to control probes and performed using Partek Genomics Suite 6.6, and any outliers were removed during quality control.

Quantitative real-time PCR (qPCR)

Splenic B cells from TLR9$^{fl/fl}$/CD19-Cre+ or TLR9$^{fl/fl}$/CD19-Cre- NOD mice (7-8-week-old) were purified using EasySep^{TM} Mouse B cell and total cellular RNA was isolated with RNeasy Mini kit (Qiagen). cDNA was synthesized using SuperScript III Firststrand synthesis kit with random hexamers (Invitrogen). qPCR was performed with Bio-Rad iQ5 qPCR detection system. The relative mRNA levels of IL-10, CD40, TIMP1, MMP19, MMP9 were determined using the 2-ΔΔCt method, by normalization with the house-keeping gene GAPDH.

Statistical analysis

Statistical analysis was performed using GraphPad Prism 7 software. Diabetes incidence was compared using log-rank test. In vitro assays were analyzed with Student's t test or ANOVA and $P < 0.05$ was considered to be statistically significant.

Results

B cell-specific TLR9 deficiency protects against T1D development

We have previously reported that total body TLR9-deficient NOD mice are protected from T1D development [24, 26]. TLR9 is highly expressed in B cells and shown to play an important role in systemic autoimmune disorders, such as SLE [31, 32]. To determine the intrinsic role of TLR9 in B cells in the immune-pathogenesis of organ-specific autoimmunity, such as T1D, we first investigated spontaneous diabetes development in TLR9$^{fl/fl}$/CD19-Cre- and TLR9$^{fl/fl}$/CD19-Cre+ NOD mice. Interestingly, B cell-specific deletion of TLR9 led to striking protection from T1D development (Fig. 1A) and insulitis (Fig.S1).

TLR9 intrinsically regulates the frequency and function of B subsets.

To investigate the effect of TLR9 deletion on B cells in a steady state, we evaluated the phenotype and function of the B cells from 6-8-week-old female TLR9$^{fl/fl}$ CD19-Cre+ and TLR9$^{fl/fl}$/CD19-Cre- NOD mice *ex vivo* (Fig.S2, gating strategy). There was a significant increase in CD1d^{+}CD5^{+} B cells in the PLN and MLN from TLR9$^{fl/fl}$/CD19-Cre+ NOD mice, compared with TLR9$^{fl/fl}$/CD19-Cre- control mice (Fig. 1B, C). CD1d^{+}CD5^{+} B cells are often also IL-10-producing B regulatory cells (B10-reg) [33, 34]. Next, we assessed the B10-regs and found that B10-regs were increased in all the lymphoid tissues examined from TLR9$^{fl/fl}$/CD19-Cre+ NOD mice, compared to TLR9$^{fl/fl}$/CD19-Cre- controls (Fig.1B, D). However, a statistically significant increase in the B10-regs was found only in the PC of TLR9$^{fl/fl}$/CD19-Cre+ NOD mice (Fig.1D). Interestingly, more IL-10-producing B cells from TLR9$^{fl/fl}$/CD19-Cre+ NOD mice expressed CD40, compared to TLR9$^{fl/fl}$/CD19-Cre- mice, specifically in the PC (Fig.1E). The absolute cell numbers of different B cell subsets were also changed accordingly (Fig.S3A-E). We also evaluated the B10-regs in 30-32-week-old, non-diabetic female mice and found a similar phenotype (Fig.1F-H).

Phenotypic analysis of young mice also revealed a significant increase in marginal zone (MZ) B cells (CD21^{high}CD23^{low}) in PLN of TLR9$^{fl/fl}$/CD19-Cre+ NOD mice, compared to the controls (Fig.S4A), whereas transitional B cells (CD21^{high}CD23^{high}) in PLN of TLR9$^{fl/fl}$/CD19-Cre+ NOD mice were significantly reduced (Fig.S4B). Akin to the phenotypic changes in TLR9$^{fl/fl}$/CD19-Cre+ NOD mice at a young age, the altered marginal zone and transitional B cells in PLN were also seen in the older non-diabetic female mice at 30-32wks (Fig. S4C-D). Interestingly, unlike the young mice, marginal zone B cells (CD21^{high}CD23^{low}) from the spleen and MLN of the older mice were decreased in TLR9$^{fl/fl}$/CD19-Cre+ NOD mice, compared to the control TLR9$^{fl/fl}$/CD19-Cre- NOD mice (Fig.S4C), whereas transitional B cells (CD21^{high}CD23^{high}) from PC of old mice were increased in TLR9$^{fl/fl}$/CD19-Cre+ NOD mice, compared to the controls (Fig.S4D). It is noteworthy that the changes of B cells in PLN remained stable regardless of the age of the mice. In addition, relating to IgM and IgD B cell subsets, we showed reduced IgM^{+}IgD^{-} B cells and increased IgM^{+}IgD^{+} B cells in the spleen (Fig.S5A-B). B cell-specific TLR9 deficiency did not affect class switching overall, however, TLR9$^{fl/fl}$ CD19-Cre+ NOD

mice showed a significant reduction of IgG, which was attributed to the reduction of IgG1 (Fig.S6). Phenotypic analysis of splenic plasmacytes revealed that there was no difference in Blimp1^{+} plasmacytes between TLR9$^{fl/fl}$/CD19-Cre+ NOD mice and the control mice (Fig.S7A-B); however, Blimp1^{-} plasmacytes were significantly reduced in TLR9$^{fl/fl}$/CD19-Cre+ NOD mice (Fig.S7C). Taken together, our data suggest that B cell-specific deletion of TLR9 significantly changes proportion of B cell subsets in the various lymphoid organs, which may lead to an immune tolerant state and contribute to diabetes protection.

B cells without TLR9 are hypo-responsive to both innate and adaptive immune stimuli

To determine the intrinsic effect of TLR9 on B cell function, we stimulated splenocytes from TLR9$^{fl/fl}$/CD19-Cre+ and TLR9$^{fl/fl}$/CD19-Cre- NOD mice (6-8 wks) with anti-CD40 (adaptive stimulus), and innate stimuli including Pam3Csk4, LPS and CpG (TLR2, TLR4 and TLR9 agonists respectively). Splenocytes from TLR9 $^{fl/fl}$/CD19-Cre+ NOD mice showed significantly impaired responses to all the stimuli, regardless of whether the cells were stimulated through adaptive or innate pathways (Fig. 2A-D). To verify that the hypo-responsiveness was due to TLR9 deficiency in B cells, we repeated the experiments using purified splenic B cells from TLR9$^{fl/fl}$/CD19-Cre+ and TLR9$^{fl/fl}$/CD19-Cre- NOD mice. We found similarly impaired responses to both innate immune and adaptive stimuli, including co-stimulation of anti-CD40 and anti-IgM (Fig. 2E-I). To assess if the hypo-response was accompanied by immune-regulatory cytokines, we measured IL-10 in the supernatants of the anti-CD40 stimulated cultures. Interestingly, we found a significant increase in IL-10 production in the culture supernatants, in which B cells from TLR9$^{fl/fl}$/CD19-Cre+ were used (Fig. 2J). Moreover, the impaired immune response of the TLR9-deficient B cells was also found in the old (30-32 wks) TLR9 $^{fl/fl}$/CD19-Cre+ NOD mice (Fig. 3A-E). IL-10 in the supernatants of anti-CD40-stimulated cultures also were significantly increased in old (30-32 wks) TLR9 $^{fl/fl}$/CD19-Cre+ NOD mice (Fig. 3F). Taken together, our data suggest that B cell-specific deficiency in TLR9 promotes a B cell hypo-responsive immune tolerant state.

TLR9 regulates the fate of IL-10-producing B cells and suppresses T cell responses.

To determine if B cell-specific deficiency of TLR9 also led to hypo-responsiveness of T cells, we stimulated purified T cells from wild-type NOD mice with anti-CD3 and anti-CD28 monoclonal antibodies, in the presence of B cells from TLR9$^{fl/fl}$/CD19-Cre+ or TLR9$^{fl/fl}$/CD19-Cre- NOD mice. Similar to the hypo-responsiveness seen in TLR9-deficient B cells, wild-type NOD splenic T cells also showed impaired response to anti-CD3 and anti-CD28 stimulation when TLR9-deficient B cells were used for the antibody cross-linking (Fig. 4A). As TLR9-deficient B cells secreted a higher level of IL-10 after stimulation (Fig.2J), we hypothesized that activated B cells from TLR9$^{fl/fl}$/CD19-Cre+ NOD mice would have increased regulatory function mediated by IL-10. To test our hypothesis, we performed two sets of experiments using anti-CD40-activated B cells from TLR9$^{fl/fl}$/CD19-Cre+ and TLR9$^{fl/fl}$/CD19-Cre- NOD mice, both in co-culture and in trans-well culture. For the former, we cultured purified B cells with and without anti-CD40, together with purified T cells from wild-type NOD mice, in the presence of anti-CD3 and anti-CD28. Similar to the results shown in Fig. 4A, the T cell response was reduced in the presence of stimulated B cells from TLR9 $^{fl/fl}$/CD19-Cre+ mice (data not shown). To determine if IL-10 played a role in the suppressed T cell response, we measured the secreted IL-10 in the culture supernatants. Similar to the earlier results (Fig.2J), we detected a higher amount of secreted IL-10 was detected in the cultures where TLR9-deficient B cells were present (Fig.4B). To determine if the suppressed T cell response was indeed due to B cells from TLR9$^{fl/fl}$/CD19-Cre+ mice rather than cell contact between B cells and T cells, we repeated the experiment using a trans-well system (Research Design and Methods). We first purified splenic B cells from TLR9$^{fl/fl}$/CD19-Cre+ and TLR9$^{fl/fl}$/CD19-Cre- NOD mice and stimulated with anti-CD40 overnight. After washing, we placed the pre-activated B cells in the trans-well inserts, with the splenic T cells and B cell-depleted APCs from wild-type NOD mice seeded in the lower wells, in the presence of anti-CD3 and anti-CD28. In this culture system, there was direct cell-cell contact between T cells and APCs from wild-type NOD mice, while B cells from TLR9$^{fl/fl}$/CD19-Cre+ and TLR9$^{fl/fl}$/CD19-Cre- NOD mice were separated from T cells by the trans-well insert. We assessed T cell proliferation by ^{3}H-thymidine incorporation and the content of secreted IL-10 in the supernatant. In line with the co-culture results, we found impaired T cell proliferation, when the pre-activated B cells in the trans-well inserts were from TLR9$^{fl/fl}$/CD19-

Cre+ NOD mice (Fig.4C). Again, T cell hypo-response was accompanied by higher IL-10 secretion by B cells from TLR9$^{fl/fl}$/CD19-Cre+ NOD mice (Fig.4D). To further confirm the role of IL-10 in suppressing the T cell response, we blocked IL-10 signaling using mAb to the IL-10 receptor in the trans-well system. As expected, blocking IL-10 signaling significantly enhanced T cell proliferation, whereas T cell responses were impaired in the presence of control IgG (Fig.4E). It is noteworthy that blockade of the IL-10 receptor also enhanced T cell proliferation when pre-activated B cells from TLR9$^{fl/fl}$/CD19-Cre- NOD mice were present, compared to control IgG (Fig.4E). To determine if the levels of IL10 in the systemic circulation were also altered by the absence of B cell-specific TLR9, we measured IL-10 in the serum samples of TLR9$^{fl/fl}$/CD19-Cre+ and TLR9$^{fl/fl}$/CD19-Cre- NOD mice. Interestingly, we found a significant increase in circulating IL-10 in TLR9$^{fl/fl}$/CD19-Cre+ NOD mice compared to TLR9$^{fl/fl}$/CD19-Cre- NOD mice regardless of age (Fig. 4F, 6-8 wks; Fig. 4G, 30-32wks). Taken together, our results demonstrate that B cell TLR9 deficiency converted B cells to IL-10-producing Bregs that suppressed T cell responses.

TLR9 deficiency in B cells confers protection against T1D development.

To determine if TLR9-deficient B cells induce suppression of islet β-cell autoimmunity, we first assessed whether B cell-specific TLR9 deficiency dampened autoreactive T cells, especially cytotoxic CD8$^+$ T cells by staining for IGRP-tetramer-specific CD8$^+$ T cells. Our results showed that the absence of B cell-specific TLR9 did not have noticeable effect on CD8 T cells including IGRP-tetramer-specific CD8$^+$ T cells (Fig. S8, A-C). Next, we assessed if B cell-specific TLR9 deficiency affected the proportion and the function of Treg cells. Interestingly, we found that the absence of B cell-specific TLR9 significantly increased the proportion of Treg cells (Fig.S9). To test if the increased Tregs contribute to diabetes protection, we adoptively transferred splenoctyes from TLR9$^{fl/fl}$/CD19-Cre+ and TLR9$^{fl/fl}$/CD19-Cre- NOD mice to *Rag*-/- NOD recipients, after depleting Tregs cells. In the absence of Tregs, diabetes development in the *Rag*-/- NOD recipients that received splenoctyes from TLR9$^{fl/fl}$/CD19-Cre+ mice was significantly delayed and reduced compared to the *Rag*-/- NOD recipients that received splenoctyes from TLR9$^{fl/fl}$/CD19-Cre- mice (Fig.5A). These results suggest that diabetes suppression in

TLR9$^{fl/fl}$/CD19-Cre+ NOD mice is not due to Tregs, despite their increase. To determine if TLR9-deficient B cells confer the diabetes suppression, we carried out a further set of adoptive transfers, in which we adoptively transferred purified splenic T cells from diabetic TLR9$^{fl/fl}$/CD19-Cre- NOD mice (wild type), together with purified splenic B cells from non-diabetic TLR9$^{fl/fl}$/CD19-Cre+ or TLR9$^{fl/fl}$/CD19-Cre- NOD mice, into *Rag*-/- NOD recipients. Diabetes development was significantly reduced in the *Rag*-/- NOD recipients that received B cells from TLR9$^{fl/fl}$/CD19-Cre+ mice, compared to the *Rag*-/- NOD recipients that received B cells from TLR9$^{fl/fl}$/CD19-Cre- NOD mice (Fig.5B). To investigate if IL-10 played a role in diabetes suppression, we isolated splenic B cells from the *Rag*-/- NOD recipients and assessed IL-10 gene expression, with or without anti-CD40 stimulation, by qPCR. In line with the results shown above, we found significantly higher IL-10 gene expression in the B cells from the *Rag*-/- NOD recipients that received B cells from TLR9$^{fl/fl}$/CD19-Cre+ mice, compared to the *Rag*-/- NOD recipients that received B cells from TLR9$^{fl/fl}$/CD19-Cre- NOD mice (Fig.5C). This was found both with and without anti-CD40 stimulation, with significantly higher IL10 gene expression in TLR9-deficient B cells compared to TLR9-sufficient B cells. Our data suggest that B cells from TLR9$^{fl/fl}$/CD19-Cre+ NOD mice exert stronger immunosuppressive function, mediated by the higher levels of the anti-inflammatory cytokine IL-10.

TLR9 regulates the cross talk between tissue inhibitor of metalloproteinase 1 (TIMP-1) and IL-10 in B cells

To determine the molecular mechanism by which IL-10 is enhanced in B10reg cells in the absence of TLR9, we performed microarray analysis using purified splenic B cells, directly ex vivo, from TLR9$^{fl/fl}$/CD19-Cre+ and TLR9$^{fl/fl}$/CD19-Cre- NOD mice. Among 3 down-regulated genes, we found that the gene expression of matrix metalloproteinase 19 (MMP-19) was strikingly lower in the spleen cells from TLR9$^{fl/fl}$/CD19-Cre+ mice (Fig.5D, Table.1), which was confirmed by qPCR (Fig.5E). Using Ingenuity Pathways Analysis (IPA, Qiagen), we identified that TLR9 and IL-10 interacted with MMP19 and that tissue inhibitors of metalloproteinases (TIMPs) could modulate these interactions (Fig.5F). In addition to their role in extracellular matrix remodeling, TIMPs also have cytokine functions affecting cell differentiation, apoptosis

and cell growth [35, 36]. As TIMPs inhibit the activities of the matrix metalloproteinases (MMPs) [37], [38], down regulation of MMPs may suggest up-regulation of TIMPs. To determine if TIMP-1 is up-regulated in TLR9-deficient B cells, with or without stimulation, we assessed the expression level of TIMP-1 by qPCR. Indeed, TIMP-1 was highly up-regulated in the activated B cells from TLR9$^{fl/fl}$/CD19-Cre+ mice, compared to their counterparts from TLR9$^{fl/fl}$/CD19-Cre- NOD mice (Fig.5G). The significant up-regulation of TIMP-1 was also seen in non-activated TLR9-deficient B cells although the scale was lower compared to the activated B cells (Fig.5G).

To further establish the cross talk of TLR9 with TIMP-1/MMP-19 and IL-10, we stimulated splenic B cells from wild-type NOD mice with CpG and assessed the gene expression level of TIMP-1, MMP19 and IL-10 by qPCR. Unstimulated B cells were used as controls. Supporting the results shown earlier, CpG stimulation resulted in lower gene expression of TIMP-1 and IL-10 (Fig.6A-B) but higher expression of MMP-19 (Fig.6C) compared to the controls. Interestingly, the expression level of CD40 paralleled IL-10 (Fig.6D), supporting our earlier results (Fig.1H). Our results suggest novel cross-talk between TLR9 and TIMP-1/MMP-19, which regulates IL-10 in B cells.

Discussion

As TLR9 is pivotal in the development of T1D [26], and is primarily expressed in B cells and plasmacytoid dendritic cells (pDCs) [39, 40], we aimed to clarify the role of TLR9 in B cells in development of spontaneous T1D. Our key finding was that B cell TLR9 plays a critical role in immune tolerance to islet beta cell autoimmunity, as TLR9 deficiency in B cells strongly protected NOD mice from T1D development. TLR9 modulated T1D susceptibility through different pathways, which included effects on B cell subsets, including MZ B cells, transitional B cells and B10-reg subsets. In the absence of TLR9 in B cells, these B cell subsets, particularly B10-reg cells were enhanced, both in frequency and function. At the molecular level, we discovered a novel regulatory network between TLR9 with TIMP1, MMP19, CD40 and the IL-10 signaling pathway. Our study confirmed an important function of B cells in influencing

immune tolerance whereby increased immune tolerance was observed in the absence of B cell TLR9.

IL-10-producing Breg (B10) cells are important in health and disease, in humans and in mouse models [41-44], and B10 cells are considered to be an indispensable contributor to the maintenance of tolerance and immune homeostasis. Previous studies suggested that CpG, a TLR9 agonist, induces B10 cells [45]. Interestingly, we found that the proportions $CD1d^{high}CD5^{high}$ B cells and IL-10-producing $CD1d^{high}CD5^{high}$ B cells in NOD mice are enhanced when B cells are deficient in TLR9. Moreover, the increase of Bregs found in our study was age independent. B cell-specific deficiency in TLR9 also altered the proportions of marginal zone and transitional B cells, namely increased marginal zone B cells and decreased transitional B cells. Whilst we have confirmed that TLR9 signaling plays an important role in formation of different effector B cell subsets [46, 47], the role of TLR9 in B cells goes beyond this. Our study demonstrated that B cell-specific deficiency of TLR9 led to an immune tolerant state, supported by B cell hypo-responsiveness to both innate and adaptive stimuli, as well as an impaired ability to promote optimal T cell responses. Moreover, B cells with B cell-specific TLR9 deletion were able to suppress both spontaneous and induced T1D development. All of these findings were associated with IL-10 production of B cells, regulated by TLR9.

Interestingly, molecular analysis of TLR9-deficient and -sufficient B cells revealed only a limited number of gene expression differences and the expression of matrix metallopeptidase 19, Mmp19, was lowest in TLR9-deficient B cells, compared to TLR9-sufficient B cells. The matrix metalloproteinase gene family includes over 20 genes that regulate the breakdown of extracellular matrix in normal physiological and disease processes [48, 49]. The expression of MMP and its inhibitor TIMP, tissue inhibitor of metalloproteinase, are essential in tissue remodeling and cell signaling [38, 50]. An earlier study showed that Mmp-19 is expressed in synovial blood vessels and in circulating T cells of patients with rheumatoid arthritis [51].
Other studies have reported that the MMP inhibitors, TIMPs, may play a role in the pathological processes in multiple sclerosis in humans [52, 53] and experimental autoimmune encephalomyelitis in animal models [54, 55]. Furthermore, Guedez and colleagues [35] have

reported that TIMP-1 regulates IL-10 in B cell differentiation in lymphoma cell lines. However, little is known about the role of MMPs in the function of TLR9 and B cell regulation. Using Ingenuity Pathway Analysis, we identified the network of TLR9-IL-10 with MMP and the MMP inhibitor TIMP-1 in B cells. TLR9-deficient B cells have a marked reduction of MMP19 but highly increased TIMP1, with or without activation. It is interesting that the expression of CD40 in TLR9-deficient B cells was positively associated with the expression of IL-10 and TIMP1 expression, but negatively associated with the expression of MMP-19. Sanchooli and colleagues [56] reported an elevation of soluble CD154 (CD40 ligand) and TIMP1 in patients with multiple sclerosis. Our study suggests a novel cross-talk loop of TLR9, MMPs/TIMP-1, IL-10 and CD40. Our results also demonstrate that TLR9 plays a vital role in this network, which leads to immune tolerance to islet β-cell autoimmunity. Thus, TLR9 in B cells acts as a crucial modulator of T1D susceptibility.

B cell depletion immunotherapy has been used for treating different autoimmune disorders with some success [57, 58]. However, B cell depletion also eliminates IL-10 producing Breg cells, which are important in immune tolerance to autoimmunity. Our study provides pre-clinical information for selective molecular therapy by targeting TLR9 in B cells.

Acknowledgements

Author Contributions: LW conceived the project. SS, JAP and LW designed the experiments. SS, JP, JAP analyzed the data and conducted experiments. YH, JH, YW and LZ conducted some of the experiments. YZ and HZ performed bioinformatics analysis on microarray. LC supervised part of the study. SS, JAP, FSW and LW wrote and edited the manuscript.

Guarantor Statement: LW is the guarantor of this work and had full access to all the data in the study and takes responsibility for the integrity of the data and the accuracy of the data analysis.

Conflict of Interest statement: None of the authors have any declaration of interest to disclose.

Funding: This work was supported by grants from National Institutes of Health (DK092882, DK100500, and P30 DK945735 to LW), by American Diabetes Association (1-14-BS-222 to

LW), and by a Juvenile Diabetes Research Foundation Postdoctoral Research Fellowship (PDF-2016-197 to JAP).

Data and Resource Availability

Data availability statements

The datasets generated during and/or analyzed during the current study are available from the corresponding author upon request.

Resource availability statements

The rodent models, antibodies, compounds, or other non-commercial reagents generated and used during the current study is available from the corresponding author upon request.

References

1. Majer O, Liu B, Barton GM: Nucleic acid-sensing TLRs: trafficking and regulation. Curr Opin Immunol 2017;44:26-33
2. Klein JC, Moses K, Zelinskyy G, Sody S, Buer J, Lang S, Helfrich I, Dittmer U, Kirschning CJ, Brandau S: Combined toll-like receptor 3/7/9 deficiency on host cells results in T-cell-dependent control of tumour growth. Nat Commun 2017;8:14600
3. Gonzalez-Navajas JM, Law J, Nguyen KP, Bhargava M, Corr MP, Varki N, Eckmann L, Hoffman HM, Lee J, Raz E: Interleukin 1 receptor signaling regulates DUBA expression and facilitates Toll-like receptor 9-driven antiinflammatory cytokine production. J Exp Med 2010;207:2799-2807
4. Iwasaki A, Medzhitov R: Toll-like receptor control of the adaptive immune responses. Nat Immunol 2004;5:987-995
5. Green NM, Marshak-Rothstein A: Toll-like receptor driven B cell activation in the induction of systemic autoimmunity. Semin Immunol 2011;23:106-112
6. Sindhava VJ, Oropallo MA, Moody K, Naradikian M, Higdon LE, Zhou L, Myles A, Green N, Nündel K, Stohl W, Schmidt AM, Cao W, Dorta-Estremera S, Kambayashi T, Marshak-Rothstein A, Cancro MP: A TLR9-dependent checkpoint governs B cell responses to DNA-containing antigens. The Journal of clinical investigation 2017;127:1651-1663
7. Puttur F, Francozo M, Solmaz G, Bueno C, Lindenberg M, Gohmert M, Swallow M, Tufa D, Jacobs R, Lienenklaus S, Kuhl AA, Borkner L, Cicin-Sain L, Holzmann B, Wagner H, Berod L, Sparwasser T: Conventional Dendritic Cells Confer Protection against Mouse Cytomegalovirus Infection via TLR9 and MyD88 Signaling. Cell Rep 2016;17:1113-1127
8. Cao W, Bover L, Cho M, Wen X, Hanabuchi S, Bao M, Rosen DB, Wang YH, Shaw JL, Du Q, Li C, Arai N, Yao Z, Lanier LL, Liu YJ: Regulation of TLR7/9 responses in plasmacytoid dendritic cells by BST2 and ILT7 receptor interaction. J Exp Med 2009;206:1603-1614
9. Santiago-Raber ML, Baudino L, Alvarez M, van Rooijen N, Nimmerjahn F, Izui S: TLR7/9-mediated monocytosis and maturation of Gr-1(hi) inflammatory monocytes towards Gr-1(lo) resting monocytes implicated in murine lupus. J Autoimmun 2011;37:171-179
10. Karper JC, Ewing MM, Habets KL, de Vries MR, Peters EA, van Oeveren-Rietdijk AM, de Boer HC, Hamming JF, Kuiper J, Kandimalla ER, La Monica N, Jukema JW, Quax PH: Blocking toll-like receptors 7 and 9 reduces postinterventional remodeling via reduced macrophage activation, foam cell formation, and migration. Arterioscler Thromb Vasc Biol 2012;32:e72-80
11. Yoshizaki A, Taniguchi T, Saigusa R, Fukasawa T, Ebata S, Numajiri H, Nakamura K, Yamashita T, Takahashi T, Toyama T, Asano Y, Tedder TF, Sato S: Nucleosome in patients with systemic sclerosis: possible association with immunological abnormalities via abnormal activation of T and B cells. Ann Rheum Dis 2016;75:1858-1865
12. Trujillo G, Meneghin A, Flaherty KR, Sholl LM, Myers JL, Kazerooni EA, Gross BH, Oak SR, Coelho AL, Evanoff H, Day E, Toews GB, Joshi AD, Schaller MA, Waters B, Jarai G, Westwick J, Kunkel SL, Martinez FJ, Hogaboam CM: TLR9 differentiates rapidly from slowly progressing forms of idiopathic pulmonary fibrosis. Science translational medicine 2010;2:57ra82

13. Lee J, Mo JH, Katakura K, Alkalay I, Rucker AN, Liu YT, Lee HK, Shen C, Cojocaru G, Shenouda S, Kagnoff M, Eckmann L, Ben-Neriah Y, Raz E: Maintenance of colonic homeostasis by distinctive apical TLR9 signalling in intestinal epithelial cells. Nature cell biology 2006;8:1327-1336
14. El Kebir D, Damlaj A, Makhezer N, Filep JG: Toll-like receptor 9 signaling regulates tissue factor and tissue factor pathway inhibitor expression in human endothelial cells and coagulation in mice. Critical care medicine 2015;43:e179-189
15. Hemmi H, Takeuchi O, Kawai T, Kaisho T, Sato S, Sanjo H, Matsumoto M, Hoshino K, Wagner H, Takeda K, Akira S: A Toll-like receptor recognizes bacterial DNA. Nature 2000;408:740-745
16. Latz E, Schoenemeyer A, Visintin A, Fitzgerald KA, Monks BG, Knetter CF, Lien E, Nilsen NJ, Espevik T, Golenbock DT: TLR9 signals after translocating from the ER to CpG DNA in the lysosome. Nature immunology 2004;5:190-198
17. Wagner H: Interactions between bacterial CpG-DNA and TLR9 bridge innate and adaptive immunity. Current opinion in microbiology 2002;5:62-69
18. Christensen SR, Shlomchik MJ: Regulation of lupus-related autoantibody production and clinical disease by Toll-like receptors. Seminars in immunology 2007;19:11-23
19. Santiago-Raber ML, Baudino L, Izui S: Emerging roles of TLR7 and TLR9 in murine SLE. Journal of autoimmunity 2009;33:231-238
20. Ehlers M, Fukuyama H, McGaha TL, Aderem A, Ravetch JV: TLR9/MyD88 signaling is required for class switching to pathogenic IgG2a and 2b autoantibodies in SLE. The Journal of experimental medicine 2006;203:553-561
21. Tao K, Fujii M, Tsukumo S, Maekawa Y, Kishihara K, Kimoto Y, Horiuchi T, Hisaeda H, Akira S, Kagami S, Yasutomo K: Genetic variations of Toll-like receptor 9 predispose to systemic lupus erythematosus in Japanese population. Annals of the rheumatic diseases 2007;66:905-909
22. Mande P, Zirak B, Ko WC, Taravati K, Bride KL, Brodeur TY, Deng A, Dresser K, Jiang Z, Ettinger R, Fitzgerald KA, Rosenblum MD, Harris JE, Marshak-Rothstein A: Fas ligand promotes an inducible TLR-dependent model of cutaneous lupus-like inflammation. The Journal of clinical investigation 2018;128:2966-2978
23. Barrat FJ, Coffman RL: Development of TLR inhibitors for the treatment of autoimmune diseases. Immunological reviews 2008;223:271-283
24. Tai N, Wong FS, Wen L: TLR9 deficiency promotes CD73 expression in T cells and diabetes protection in nonobese diabetic mice. Journal of immunology (Baltimore, Md : 1950) 2013;191:2926-2937
25. Zhang Y, Lee AS, Shameli A, Geng X, Finegood D, Santamaria P, Dutz JP: TLR9 blockade inhibits activation of diabetogenic CD8+ T cells and delays autoimmune diabetes. Journal of immunology (Baltimore, Md : 1950) 2010;184:5645-5653
26. Liu M, Peng J, Tai N, Pearson JA, Hu C, Guo J, Hou L, Zhao H, Wong FS, Wen L: Toll-like receptor 9 negatively regulates pancreatic islet beta cell growth and function in a mouse model of type 1 diabetes. Diabetologia 2018;61:2333-2343
27. Rivera-Correa J, Guthmiller JJ, Vijay R, Fernandez-Arias C, Pardo-Ruge MA, Gonzalez S, Butler NS, Rodriguez A: Plasmodium DNA-mediated TLR9 activation of T-bet B cells contributes to autoimmune anaemia during malaria. Nature communications 2017;8:1282

28. Iwata S, Yamaoka K, Niiro H, Nakano K, Wang SP, Akashi K, Tanaka Y: Amplification of Toll-like receptor-mediated signaling through spleen tyrosine kinase in human B-cell activation. The Journal of allergy and clinical immunology 2012;129:1594-1601.e1592
29. Yu JE, Knight AK, Radigan L, Marron TU, Zhang L, Sanchez-Ramón S, Cunningham-Rundles C: Toll-like receptor 7 and 9 defects in common variable immunodeficiency. The Journal of allergy and clinical immunology 2009;124:349-356, 356.e341-343
30. Capolunghi F, Rosado MM, Cascioli S, Girolami E, Bordasco S, Vivarelli M, Ruggiero B, Cortis E, Insalaco A, Fantò N, Gallo G, Nucera E, Loiarro M, Sette C, De Santis R, Carsetti R, Ruggiero V: Pharmacological inhibition of TLR9 activation blocks autoantibody production in human B cells from SLE patients. Rheumatology (Oxford, England) 2010;49:2281-2289
31. Guiducci C, Gong M, Xu Z, Gill M, Chaussabel D, Meeker T, Chan JH, Wright T, Punaro M, Bolland S, Soumelis V, Banchereau J, Coffman RL, Pascual V, Barrat FJ: TLR recognition of self nucleic acids hampers glucocorticoid activity in lupus. Nature 2010;465:937-941
32. Christensen SR, Shupe J, Nickerson K, Kashgarian M, Flavell RA, Shlomchik MJ: Toll-like receptor 7 and TLR9 dictate autoantibody specificity and have opposing inflammatory and regulatory roles in a murine model of lupus. Immunity 2006;25:417-428
33. Piper CJM, Rosser EC, Oleinika K, Nistala K, Krausgruber T, Rendeiro AF, Banos A, Drozdov I, Villa M, Thomson S, Xanthou G, Bock C, Stockinger B, Mauri C: Aryl Hydrocarbon Receptor Contributes to the Transcriptional Program of IL-10-Producing Regulatory B Cells. Cell reports 2019;29:1878-1892.e1877
34. Lykken JM, Candando KM, Tedder TF: Regulatory B10 cell development and function. International immunology 2015;27:471-477
35. Guedez L, Mansoor A, Birkedal-Hansen B, Lim MS, Fukushima P, Venzon D, Stetler-Stevenson WG, Stetler-Stevenson M: Tissue inhibitor of metalloproteinases 1 regulation of interleukin-10 in B-cell differentiation and lymphomagenesis. Blood 2001;97:1796-1802
36. Zajac E, Schweighofer B, Kupriyanova TA, Juncker-Jensen A, Minder P, Quigley JP, Deryugina EI: Angiogenic capacity of M1- and M2-polarized macrophages is determined by the levels of TIMP-1 complexed with their secreted proMMP-9. Blood 2013;122:4054-4067
37. Levin M, Udi Y, Solomonov I, Sagi I: Next generation matrix metalloproteinase inhibitors - Novel strategies bring new prospects. Biochimica et biophysica acta Molecular cell research 2017;1864:1927-1939
38. Sampieri CL, Nuttall RK, Young DA, Goldspink D, Clark IM, Edwards DR: Activation of p38 and JNK MAPK pathways abrogates requirement for new protein synthesis for phorbol ester mediated induction of select MMP and TIMP genes. Matrix biology : journal of the International Society for Matrix Biology 2008;27:128-138
39. Bialecki E, Paget C, Fontaine J, Capron M, Trottein F, Faveeuw C: Role of marginal zone B lymphocytes in invariant NKT cell activation. Journal of immunology (Baltimore, Md : 1950) 2009;182:6105-6113
40. Ouabed A, Hubert FX, Chabannes D, Gautreau L, Heslan M, Josien R: Differential control of T regulatory cell proliferation and suppressive activity by mature plasmacytoid versus conventional spleen dendritic cells. Journal of immunology (Baltimore, Md : 1950) 2008;180:5862-5870
41. van de Veen W, Stanic B, Yaman G, Wawrzyniak M, Söllner S, Akdis DG, Rückert B, Akdis CA, Akdis M: IgG4 production is confined to human IL-10-producing regulatory B cells

that suppress antigen-specific immune responses. The Journal of allergy and clinical immunology 2013;131:1204-1212
42. Mauri C, Blair PA: Regulatory B cells in autoimmunity: developments and controversies. Nature reviews Rheumatology 2010;6:636-643
43. Amu S, Saunders SP, Kronenberg M, Mangan NE, Atzberger A, Fallon PG: Regulatory B cells prevent and reverse allergic airway inflammation via FoxP3-positive T regulatory cells in a murine model. The Journal of allergy and clinical immunology 2010;125:1114-1124.e1118
44. Vonberg AD, Acevedo-Calado M, Cox AR, Pietropaolo SL, Gianani R, Lundy SK, Pietropaolo M: CD19+IgM+ cells demonstrate enhanced therapeutic efficacy in type 1 diabetes mellitus. JCI Insight 2018;3 (23): e99860
45. Schleimann MH, Kobberø ML, Vibholm LK, Kjær K, Giron LB, Busman-Sahay K, Chan CN, Nekorchuk M, Schmidt M, Wittig B, Damsgaard TE, Ahlburg P, Hellfritzsch MB, Zuwala K, Rothemejer FH, Olesen R, Schommers P, Klein F, Dweep H, Kossenkov A, Nyengaard JR, Estes JD, Abdel-Mohsen M, Østergaard L, Tolstrup M, Søgaard OS, Denton PW: TLR9 agonist MGN1703 enhances B cell differentiation and function in lymph nodes. EBioMedicine 2019;45:328-340
46. Guerrier T, Youinou P, Pers JO, Jamin C: TLR9 drives the development of transitional B cells towards the marginal zone pathway and promotes autoimmunity. Journal of autoimmunity 2012;39:173-179
47. Green EA, Eynon EE, Flavell RA: Local expression of TNFalpha in neonatal NOD mice promotes diabetes by enhancing presentation of islet antigens. Immunity 1998;9:733-743
48. Jackson BC, Nebert DW, Vasiliou V: Update of human and mouse matrix metalloproteinase families. Human genomics 2010;4:194-201
49. Ries C: Cytokine functions of TIMP-1. Cellular and molecular life sciences : CMLS 2014;71:659-672
50. Sanchavanakit N, Saengtong W, Manokawinchoke J, Pavasant P: TNF-α stimulates MMP-3 production via PGE2 signalling through the NF-kB and p38 MAPK pathway in a murine cementoblast cell line. Archives of oral biology 2015;60:1066-1074
51. Kolb C, Mauch S, Peter HH, Krawinkel U, Sedlacek R: The matrix metalloproteinase RASI-1 is expressed in synovial blood vessels of a rheumatoid arthritis patient. Immunol Lett 1997;57:83-88
52. Kaushik DK, Hahn JN, Yong VW: EMMPRIN, an upstream regulator of MMPs, in CNS biology. Matrix biology : journal of the International Society for Matrix Biology 2015;null:138-146
53. Leppert D, Ford J, Stabler G, Grygar C, Lienert C, Huber S, Miller KM, Hauser SL, Kappos L: Matrix metalloproteinase-9 (gelatinase B) is selectively elevated in CSF during relapses and stable phases of multiple sclerosis. Brain : a journal of neurology 1998;null:2327-2334
54. Ben-Hur T, Ben-Yosef Y, Mizrachi-Kol R, Ben-Menachem O, Miller A: Cytokine-mediated modulation of MMPs and TIMPs in multipotential neural precursor cells. Journal of neuroimmunology 2006;175:12-18
55. Thorne M, Moore CS, Robertson GS: Lack of TIMP-1 increases severity of experimental autoimmune encephalomyelitis: Effects of darbepoetin alfa on TIMP-1 null and wild-type mice. Journal of neuroimmunology 2009;211:92-100

56. Sanchooli J, Ramroodi N, Sanadgol N, Sarabandi V, Ravan H, Rad RS: Relationship between metalloproteinase 2 and 9 concentrations and soluble CD154 expression in Iranian patients with multiple sclerosis. The Kaohsiung journal of medical sciences 2014;30:235-242
57. Pescovitz MD, Greenbaum CJ, Krause-Steinrauf H, Becker DJ, Gitelman SE, Goland R, Gottlieb PA, Marks JB, McGee PF, Moran AM, Raskin P, Rodriguez H, Schatz DA, Wherrett D, Wilson DM, Lachin JM, Skyler JS, Type 1 Diabetes TrialNet Anti CDSG: Rituximab, B-lymphocyte depletion, and preservation of beta-cell function. N Engl J Med 2009;361:2143-2152
58. Quintana L, Paniagua JA, Gil-Contreras D, Jimenez-Yuste V, Torres A, Velasco F: Improving type 1 diabetes after treatment of immune thrombocytopenia with rituximab: killing two birds with one stone. Diabetes Care 2010;33:e122

Tables

Table 1. Significant microarray data from purified splenic B cells.

Gene.Symbol	RefSeq	TLR9-sufficient B cell gene express	TLR9-deficient B gene expressio	Fold Change	P.value
Gm20257	NR_045007	7.07757	5.510315	0.33745	6.40E-07
Mmp19	NM_001164197	8.27076	4.308635	0.064163	1.38E-06
Tlr9	NM_031178	9.067313	5.851875	0.107661	1.68E-06
Pde3b	NM_011055	7.112163	8.42422	2.482953	2.63E-06
Snora30	NR_034045	6.635437	8.76151	4.365277	3.91E-06

Figure legends

Figure 1 –B cell-specific TLR9 deficiency protected against T1D by altering the frequency and function of B subsets.

A. TLR9$^{fl/fl}$CD19-Cre- NOD mice and TLR9$^{fl/fl}$CD19-Cre+ NOD littermates were observed for spontaneous diabetes, from 10 weeks of age. Diabetes development was assessed by testing weekly for glycosuria, and confirmed by measuring blood glucose (250mg/dl (13.9mmol/L)). **B.** Representative flow cytometric plots gated on single, live cells expressing B220^{+}TCRbeta^{-} and then gated as a quadrant on CD1d vs CD5 and IL-10. **C-E** demonstrate 6-8-week-old female mice (*n*=7/per group); **C** shows a graphical summary of flow cytometric analysis of B cells expressing CD1d^{+}CD5^{+}, while **D** and **E**, shows graphical summaries of the frequency of B cells expressing IL-10^{+} and IL-10^{+}CD40^{+}. **F-H** demonstrate 30-32week old non-diabetic female mice (*n*=4/per group); **F** shows a graphical summary of flow cytometric analysis of B cells expressing CD1d^{+}CD5^{+}, while **G** and **H**, show graphical summaries of B cells expressing IL-10^{+}and IL-10^{+}CD40^{+}. Data were pooled from 2 independent experiments and assessed for significance using a Student's T Test or 2-way ANOVA **(C-H)**. **A** was assessed for significance using a log-rank (Mantel-Cox) test.

Figure 2 –B cells without TLR9 are hypo-responsive to both innate and adaptive immune stimuli in 6-8-week-old mice.

Cell proliferation was assessed by ^{3}H-thymidine incorporation, added at 48 hours, and was incubated with the cells for 18 hours prior to harvest. Data are presented as counts per minute (CPM) with the background subtracted (cells without stimulation). **A-D**. Total splenocytes from both TLR9$^{fl/fl}$CD19-Cre- NOD mice and TLR9$^{fl/fl}$CD19-Cre+ NOD mice were stimulated in the presence of various concentrations of anti-CD40, Pam3csk4, LPS and CpG (*n*=3/per group). **E-I**. Splenic B cells from 6-8-week-old female TLR9$^{fl/fl}$ CD19-Cre- NOD mice and TLR9$^{fl/fl}$ CD19-Cre+ NOD mice were isolated and stimulated in the presence of various concentrations of anti-CD40 and IgM/anti-CD40, Pam3Csk4, LPS and CpG (*n*=3-5/per group). **J**, shows IL-10 in supernatants removed from the anti-CD40 cultures in **E** at 48 hours (*n*=5/per group). Data shown

were pooled from 2 independent experiments and assessed for significance using a Student's T Test or 2-way ANOVA.

Figure 3 –B cells without TLR9 are also hypo-responsive to both innate and adaptive immune stimuli in 30-32-week-old non-diabetic mice.

A-E, Splenic B cells from both TLR9$^{fl/fl}$CD19-Cre- NOD mice and TLR9$^{fl/fl}$CD19-Cre+ NOD mice were isolated and stimulated in the presence of various concentrations of anti-CD40 and IgM/anti-CD40, Pam3Csk4, LPS and CpG in 30-32- week-old non-diabetic female mice (*n*=3/per group). **F**, supernatants removed from the anti-CD40 cultures in **A** at 48 hours were tested for IL-10 by ELISA (*n*=3-6/per group). Proliferation was assessed by ^{3}H-thymidine incorporation, added at 48 hours and incubated with cells for 18 hours. Data are presented as counts per minute (CPM), with the background subtracted (cells without stimulation). Data shown were pooled from 2 independent experiments and assessed for significance using a Student's T Test or 2-way ANOVA.

Figure 4 –TLR9 regulates the fate of IL-10-producing B cells.

A, proliferation of T cells; total splenic B cells from both TLR9$^{fl/fl}$CD19-Cre- NOD and TLR9$^{fl/fl}$CD19-Cre+ NOD mouse spleens (stimulated by anti-CD40, 6-8-week-old female mice) co-cultured with T cells from 6-8-week-old female wild-type NOD mice with anti-CD3 and anti-CD28 in co-culture with background counts subtracted (from cultures without B cells) (*n*=3-4/per group). **B**, supernatants removed from the culture in **A** at 48 hours were tested for IL-10 by ELISA (*n*=4/per group). **C** shows proliferation of T cells; total splenic B cells from both 6-8-week-old TLR9$^{fl/fl}$CD19-Cre- NOD and TLR9$^{fl/fl}$CD19-Cre+ NOD mice were stimulated by anti-CD40 in inserts with T cells from 6-8-week-old female wild-type NOD mice in the bottom chamber with anti-CD3 and anti-CD28, in a transwell system (*n*=7-8/per group). **D,** supernatants removed from the cultures in **C** at 48 hours were tested for IL-10 by ELISA (*n*=6/per group). **E** shows proliferation of T cells with either the IL-10 receptor blocking mAb or control IgG added into co-culture transwell system (*n*=6/per group). Proliferation was assessed by ^{3}H-thymidine incorporation, added at 48 hours and incubated with the T cells for 18 hours. **F**, serum from both 6-8-week-old female TLR9$^{fl/fl}$CD19-Cre- NOD mice and TLR9$^{fl/fl}$CD19-Cre+ NOD mice were

tested for IL-10 by ELISA (*n*=11-12/per group). **G**, serum from both 30-32-week-old female TLR9$^{fl/fl}$CD19-Cre- NOD and TLR9$^{fl/fl}$CD19-Cre+ NOD mice were tested for IL-10 by ELISA (*n*=6-9/per group). Data shown were pooled from 2 independent experiments and assessed for significance using a Student's T Test or 2-way ANOVA. The final concentration of anti-CD3 was 1:400, with 1μg /ml anti-CD28.

Figure 5 –TLR9 deficiency in B cells confers protection against T1D development.

A, Spontaneous diabetes in *Rag-/-* NOD mice (females, 4-5 weeks old) following adoptive transfer of Treg–depleted splenocytes (8x10^7/mouse) from TLR9$^{fl/fl}$CD19-Cre- NOD and TLR9$^{fl/fl}$CD19-Cre+ NOD mice (females. 6-8 weeks old). Diabetes was assessed by weekly glycosuria testing and confirmed after blood glucose testing (250mg/dl (13.9mmol/L)) (*n*=6/per group). **B,** Spontaneous diabetes in *Rag-/-* NOD mice (females, 4-5 weeks old) following adoptive transfer of purified T cells (5x10^6/mouse) from diabetic TLR9$^{fl/fl}$CD19-Cre- NOD mice together with purified splenic B cells (5x10^6/mouse) from non-diabetic TLR9$^{fl/fl}$CD19-Cre- NOD and TLR9$^{fl/fl}$CD19-Cre+ NOD mice (females, 6-8 weeks old). Diabetes was assessed by weekly glycosuria testing and confirmed after blood glucose testing (250mg/dl (13.9mmol/L)) (*n*=9-13/per group). **C**, the levels of IL-10 mRNA in splenic B cells from TLR9$^{fl/fl}$CD19-Cre- NOD mice and TLR9$^{fl/fl}$CD19-Cre+ NOD mice with (left) and without (right) anti-CD40 stimulation (*n*=3-6/per group). **D,** microarray heat map showing averaged and normalized gene expression from purified splenic B cells from TLR9$^{fl/fl}$CD19-Cre- NOD mice and TLR9$^{fl/fl}$CD19-Cre+ NOD mice (6-8-week-old female mice) (*n*=3/per group). Averaged gene expression values are plotted based on the data ranges, where the lower expression is represented in blue, while higher gene expression is represented in red. **E,** the microarray levels of MMP19 in isolated splenic B cells without anti-CD40 stimulation from TLR9$^{fl/fl}$CD19-Cre- NOD mice and TLR9$^{fl/fl}$CD19-Cre+ NOD mice (6-8-week-old, female mice) (*n*=3/per group). **F,** gene network identified using IPA analysis. Dashed lines indicate indirect interactions, while solid lines indicate direct interactions. Arrow indicates direction of signaling pathway. **G,** the levels of TIMP-1 mRNA in isolated splenic B cells with (left) and without (right) anti-CD40 stimulation from TLR9$^{fl/fl}$CD19-Cre- NOD mice and TLR9$^{fl/fl}$CD19-Cre+ NOD mice (6-8-week-old, female mice) (*n*=3-6/per group). **A-B,** Log-rank (Mantel-cox) test was used for statistical analysis. Data were pooled from 2

independent experiments. Data shown in **C**, **E** and **G** were pooled from 2-3 independent experiments and assessed for significance using a Student's T Test.

Figure 6 –TLR9 regulates the cross talk between tissue inhibitor of metalloproteinase 1 (TIMP1) and IL-10 signaling pathways in B cells.

A-D, the levels of TIMP1, IL-10, MMP19 and CD40 mRNA from CpG-stimulated (10ng/ml) isolated splenic B cells from 6-8-week-old, female $TLR9^{fl/fl}$CD19-Cre- NOD and $TLR9^{fl/fl}$CD19-Cre+ NOD mice (*n*=3-6/per group). Data shown were pooled from 2-3 independent experiments and assessed for significance using a Student's T Test.

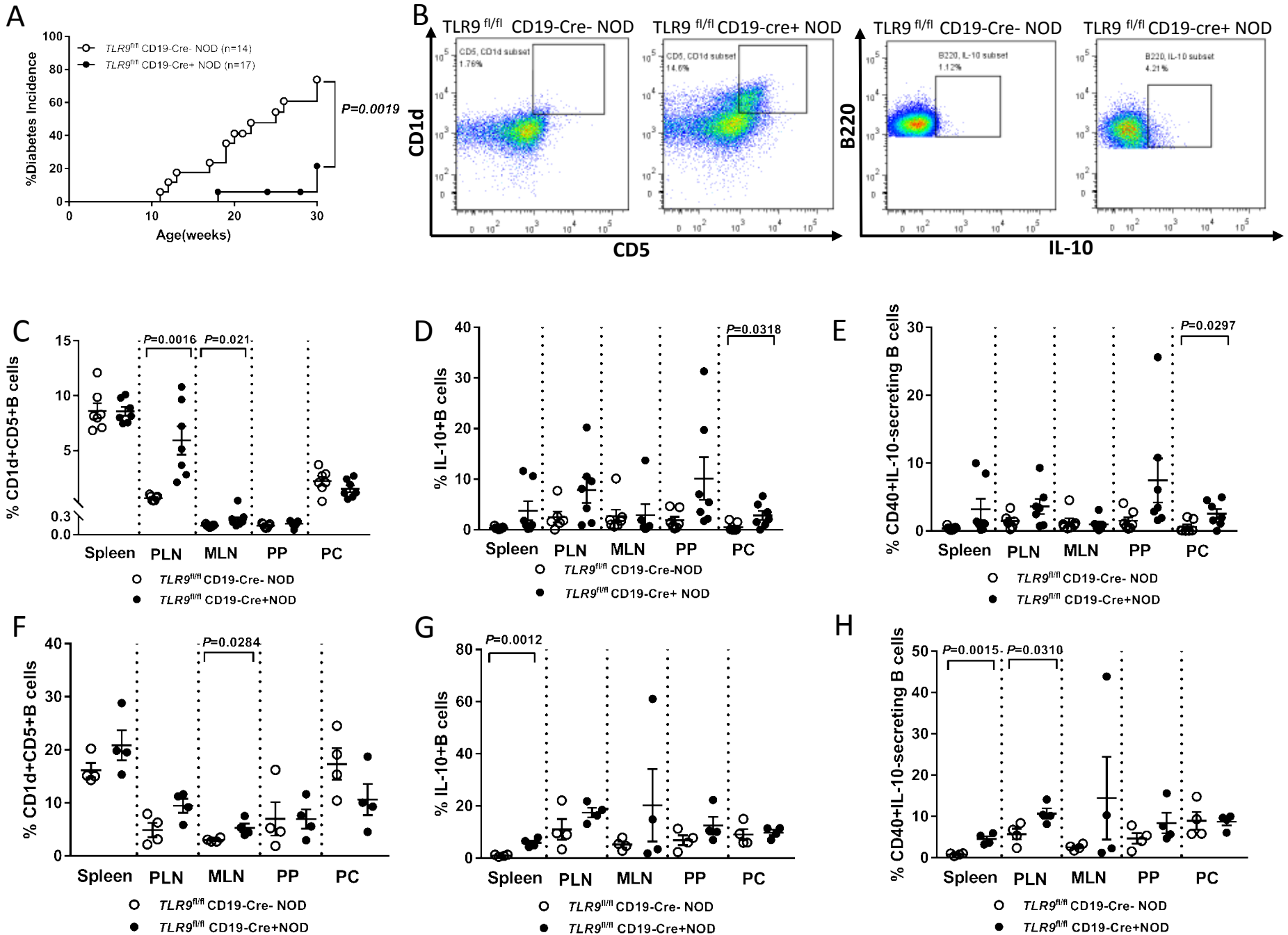
A
%Diabetes Incidence
Age(weeks)
TLR9fl/fl CD19-Cre- NOD (n=14)
TLR9fl/fl CD19-Cre+ NOD (n=17)
P=0.0019
B
TLR9 fl/fl CD19-Cre- NOD
TLR9 fl/fl CD19-cre+ NOD
CD1d
CD5
B220
IL-10
C
% CD1d+CD5+B cells
P=0.0016
P=0.021
Spleen PLN MLN PP PC
TLR9fl/fl CD19-Cre- NOD
TLR9fl/fl CD19-Cre+NOD
D
% IL-10+B cells
P=0.0318
TLR9fl/fl CD19-Cre-NOD
TLR9fl/fl CD19-Cre+ NOD
E
% CD40+IL-10-secreting B cells
P=0.0297
F
% CD1d+CD5+B cells
P=0.0284
G
% IL-10+B cells
P=0.0012
H
% CD40+IL-10-secreting B cells
P=0.0015
P=0.0310

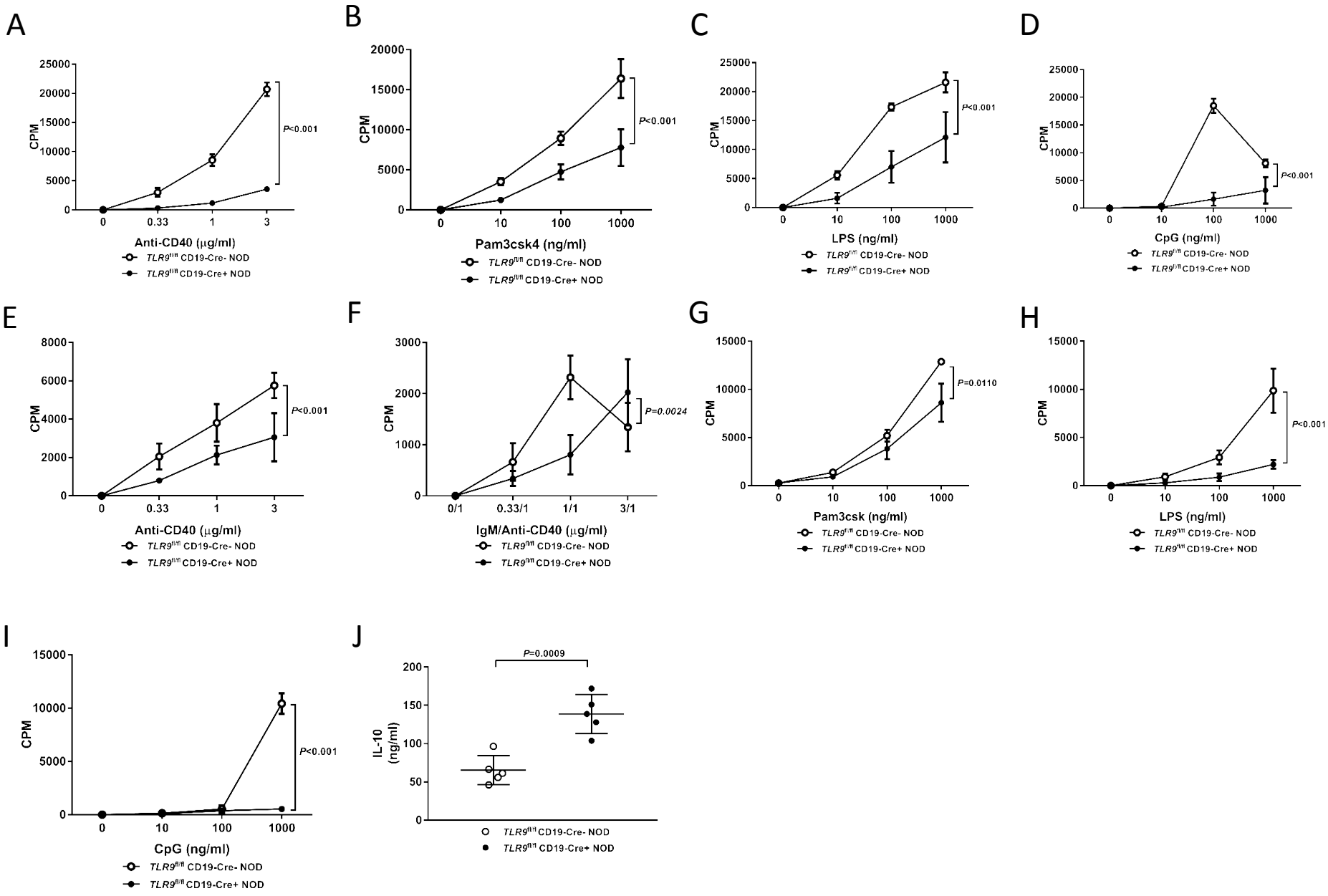
A
CPM
25000
20000
15000
10000
5000
0
P<0.001
0
0.33
1
3
Anti-CD40 (μg/ml)
TLR9fl/fl CD19-Cre- NOD
TLR9fl/fl CD19-Cre+ NOD
B
CPM
20000
15000
10000
5000
0
P<0.001
0
10
100
1000
Pam3csk4 (ng/ml)
TLR9fl/fl CD19-Cre- NOD
TLR9fl/fl CD19-Cre+ NOD
C
CPM
25000
20000
15000
10000
5000
0
P<0.001
0
10
100
1000
LPS (ng/ml)
TLR9fl/fl CD19-Cre- NOD
TLR9fl/fl CD19-Cre+ NOD
D
CPM
25000
20000
15000
10000
5000
0
P<0.001
0
10
100
1000
CpG (ng/ml)
TLR9fl/fl CD19-Cre- NOD
TLR9fl/fl CD19-Cre+ NOD
E
CPM
8000
6000
4000
2000
0
P<0.001
0
0.33
1
3
Anti-CD40 (μg/ml)
TLR9fl/fl CD19-Cre- NOD
TLR9fl/fl CD19-Cre+ NOD
F
CPM
3000
2000
1000
0
P=0.0024
0/1
0.33/1
1/1
3/1
IgM/Anti-CD40 (μg/ml)
TLR9fl/fl CD19-Cre- NOD
TLR9fl/fl CD19-Cre+ NOD
G
CPM
15000
10000
5000
0
P=0.0110
0
10
100
1000
Pam3csk (ng/ml)
TLR9fl/fl CD19-Cre- NOD
TLR9fl/fl CD19-Cre+ NOD
H
CPM
15000
10000
5000
0
P<0.001
0
10
100
1000
LPS (ng/ml)
TLR9fl/fl CD19-Cre- NOD
TLR9fl/fl CD19-Cre+ NOD
I
CPM
15000
10000
5000
0
P<0.001
0
10
100
1000
CpG (ng/ml)
TLR9fl/fl CD19-Cre- NOD
TLR9fl/fl CD19-Cre+ NOD
J
IL-10 (ng/ml)
200
150
100
50
0
P=0.0009
TLR9fl/fl CD19-Cre- NOD
TLR9fl/fl CD19-Cre+ NOD

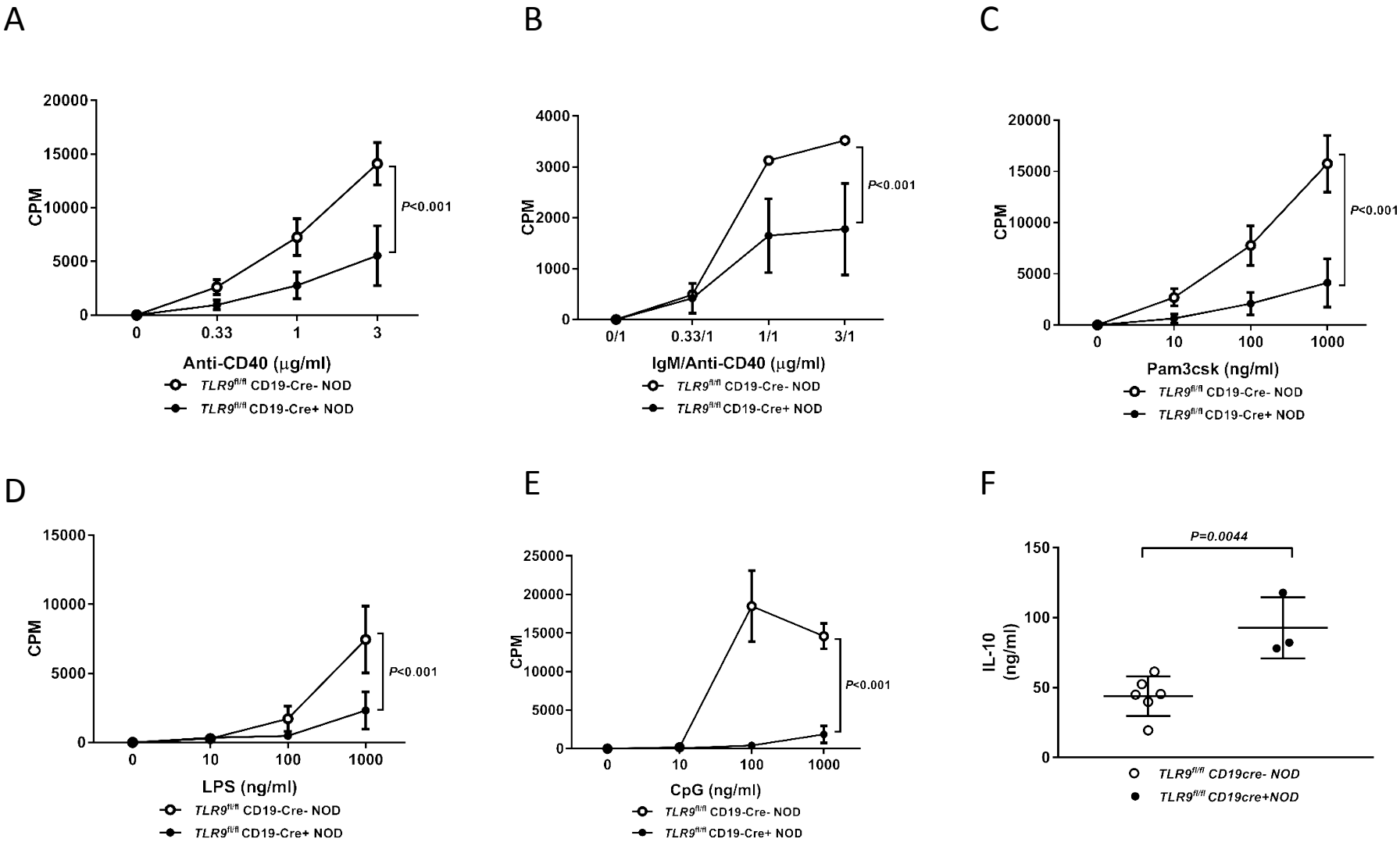
A
20000
15000
10000
5000
0
CPM
P<0.001
0
0.33
1
3
Anti-CD40 (μg/ml)
TLR9fl/fl CD19-Cre- NOD
TLR9fl/fl CD19-Cre+ NOD
B
4000
3000
2000
1000
0
CPM
P<0.001
0/1
0.33/1
1/1
3/1
IgM/Anti-CD40 (μg/ml)
TLR9fl/fl CD19-Cre- NOD
TLR9fl/fl CD19-Cre+ NOD
C
20000
15000
10000
5000
0
CPM
P<0.001
0
10
100
1000
Pam3csk (ng/ml)
TLR9fl/fl CD19-Cre- NOD
TLR9fl/fl CD19-Cre+ NOD
D
15000
10000
5000
0
CPM
P<0.001
0
10
100
1000
LPS (ng/ml)
TLR9fl/fl CD19-Cre- NOD
TLR9fl/fl CD19-Cre+ NOD
E
25000
20000
15000
10000
5000
0
CPM
P<0.001
0
10
100
1000
CpG (ng/ml)
TLR9fl/fl CD19-Cre- NOD
TLR9fl/fl CD19-Cre+ NOD
F
P=0.0044
150
100
50
0
IL-10 (ng/ml)
TLR9fl/fl CD19cre- NOD
TLR9fl/fl CD19cre+NOD

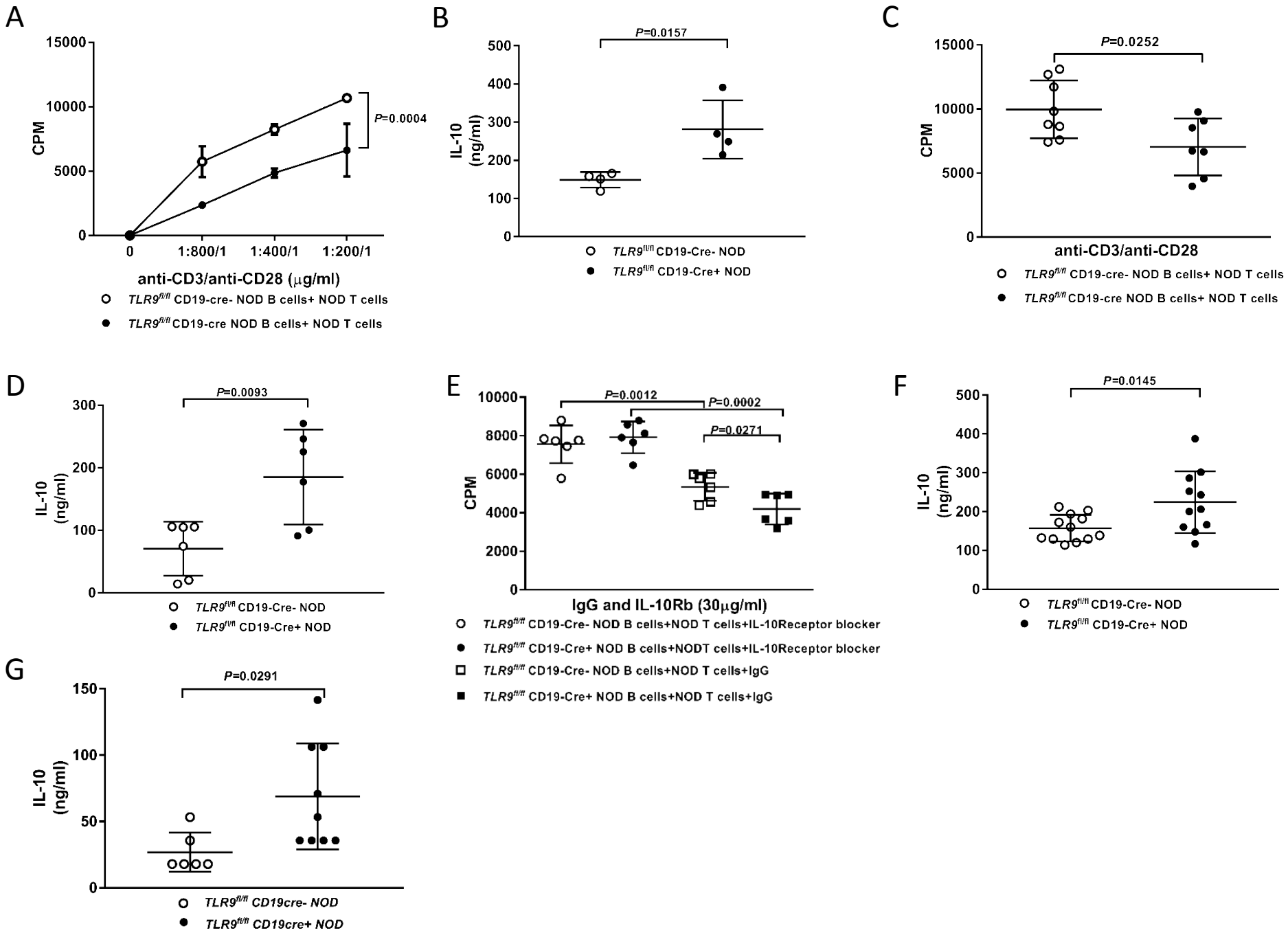
A
15000
10000
5000
0
CPM
P=0.0004
0
1:800/1
1:400/1
1:200/1
anti-CD3/anti-CD28 (μg/ml)
TLR9fl/fl CD19-cre- NOD B cells+ NOD T cells
TLR9fl/fl CD19-cre NOD B cells+ NOD T cells
B
P=0.0157
500
400
300
200
100
0
IL-10 (ng/ml)
TLR9fl/fl CD19-Cre- NOD
TLR9fl/fl CD19-Cre+ NOD
C
P=0.0252
15000
10000
5000
0
CPM
anti-CD3/anti-CD28
TLR9fl/fl CD19-cre- NOD B cells+ NOD T cells
TLR9fl/fl CD19-cre NOD B cells+ NOD T cells
D
P=0.0093
300
200
100
0
IL-10 (ng/ml)
TLR9fl/fl CD19-Cre- NOD
TLR9fl/fl CD19-Cre+ NOD
E
P=0.0012
P=0.0002
P=0.0271
10000
8000
6000
4000
2000
0
CPM
IgG and IL-10Rb (30μg/ml)
TLR9fl/fl CD19-Cre- NOD B cells+NOD T cells+IL-10Receptor blocker
TLR9fl/fl CD19-Cre+ NOD B cells+NODT cells+IL-10Receptor blocker
TLR9fl/fl CD19-Cre- NOD B cells+NOD T cells+IgG
TLR9fl/fl CD19-Cre+ NOD B cells+NOD T cells+IgG
F
P=0.0145
500
400
300
200
100
0
IL-10 (ng/ml)
TLR9fl/fl CD19-Cre- NOD
TLR9fl/fl CD19-Cre+ NOD
G
P=0.0291
150
100
50
0
IL-10 (ng/ml)
TLR9fl/fl CD19cre- NOD
TLR9fl/fl CD19cre+ NOD

Figure 5

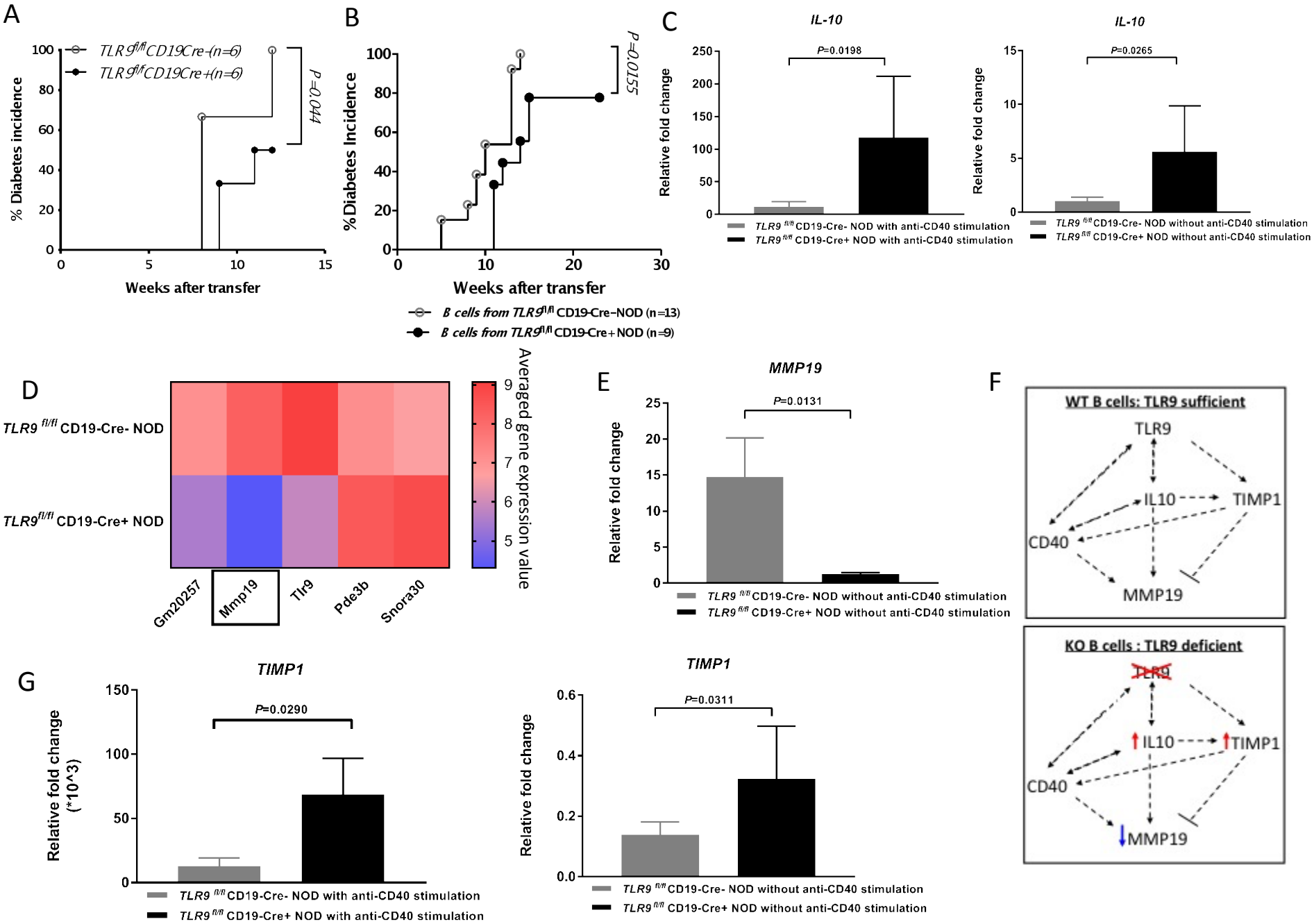
A
% Diabetes incidence
Weeks after transfer
TLR9fl/flCD19Cre-(n=6)
TLR9fl/flCD19Cre+(n=6)
P=0.044
B
%Diabetes Incidence
Weeks after transfer
P=0.0155
B cells from TLR9fl/fl CD19-Cre-NOD (n=13)
B cells from TLR9fl/fl CD19-Cre+NOD (n=9)
C
IL-10
Relative fold change
P=0.0198
TLR9 fl/fl CD19-Cre- NOD with anti-CD40 stimulation
TLR9 fl/fl CD19-Cre+ NOD with anti-CD40 stimulation
IL-10
Relative fold change
P=0.0265
TLR9 fl/fl CD19-Cre- NOD without anti-CD40 stimulation
TLR9 fl/fl CD19-Cre+ NOD without anti-CD40 stimulation
D
TLR9 fl/fl CD19-Cre- NOD
TLR9fl/fl CD19-Cre+ NOD
Gm20257
Mmp19
Tlr9
Pde3b
Snora30
Averaged gene expression value
E
MMP19
Relative fold change
P=0.0131
TLR9 fl/fl CD19-Cre- NOD without anti-CD40 stimulation
TLR9 fl/fl CD19-Cre+ NOD without anti-CD40 stimulation
F
WT B cells: TLR9 sufficient
TLR9
IL10
TIMP1
CD40
MMP19
KO B cells : TLR9 deficient
TLR9
IL10
TIMP1
CD40
MMP19
G
TIMP1
Relative fold change (*10^3)
P=0.0290
TLR9 fl/fl CD19-Cre- NOD with anti-CD40 stimulation
TLR9 fl/fl CD19-Cre+ NOD with anti-CD40 stimulation
TIMP1
Relative fold change
P=0.0311
TLR9 fl/fl CD19-Cre- NOD without anti-CD40 stimulation
TLR9 fl/fl CD19-Cre+ NOD without anti-CD40 stimulation

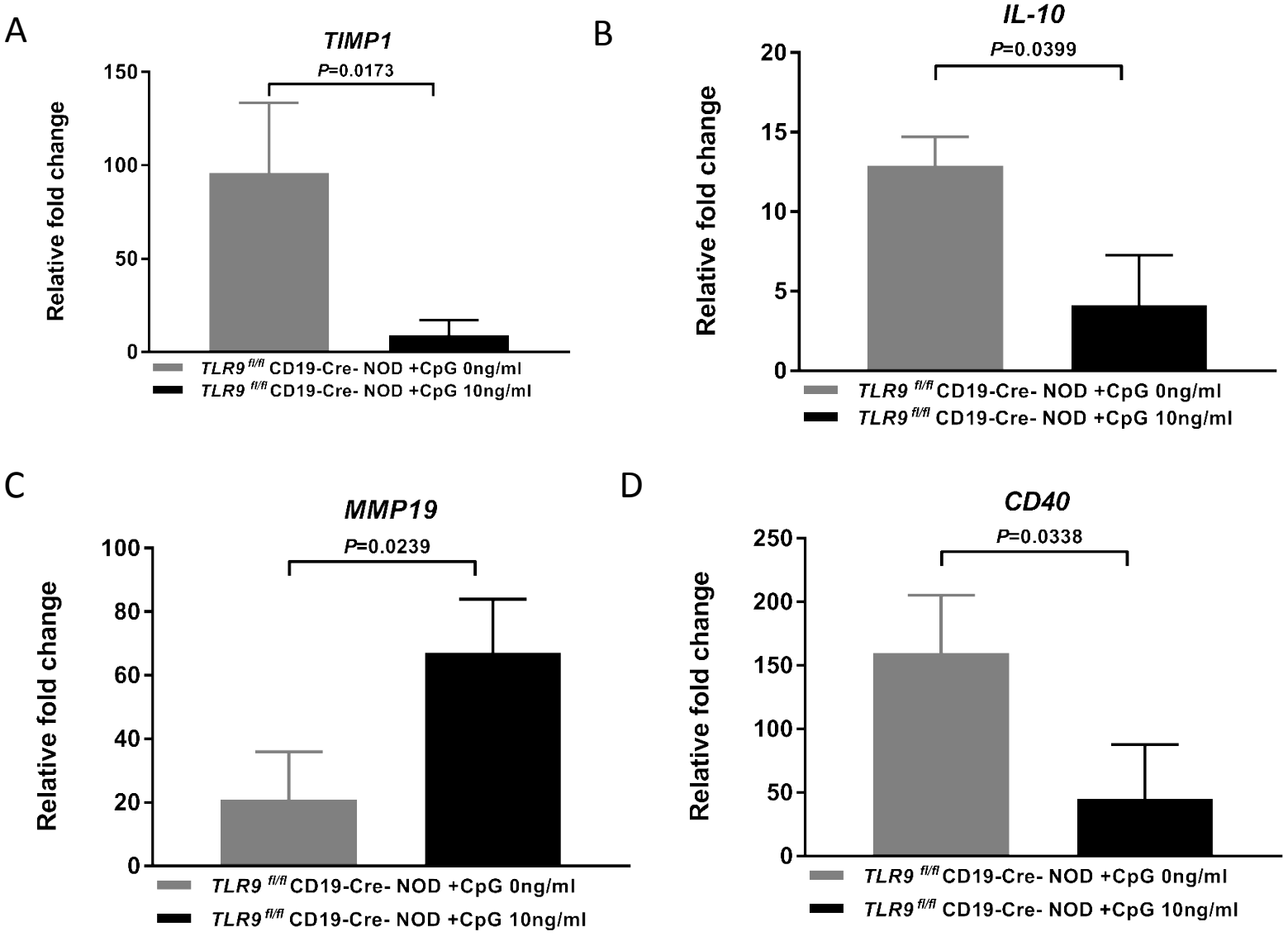
A
TIMP1
P=0.0173
Relative fold change
150
100
50
0
TLR9 fl/fl CD19-Cre- NOD +CpG 0ng/ml
TLR9 fl/fl CD19-Cre- NOD +CpG 10ng/ml
B
IL-10
P=0.0399
Relative fold change
20
15
10
5
0
TLR9 fl/fl CD19-Cre- NOD +CpG 0ng/ml
TLR9 fl/fl CD19-Cre- NOD +CpG 10ng/ml
C
MMP19
P=0.0239
Relative fold change
100
80
60
40
20
0
TLR9 fl/fl CD19-Cre- NOD +CpG 0ng/ml
TLR9 fl/fl CD19-Cre- NOD +CpG 10ng/ml
D
CD40
P=0.0338
Relative fold change
250
200
150
100
50
0
TLR9 fl/fl CD19-Cre- NOD +CpG 0ng/ml
TLR9 fl/fl CD19-Cre- NOD +CpG 10ng/ml

Supplementary Figure Legends

Figure S1 – B cell-specific TLR9 deficiency protected NOD mice from developing insulitis. Pancreata from 20-wk-old female *TLR9*$^{fl/fl}$/CD19-Cre- and *TLR9*$^{fl/fl}$/CD19-Cre-+ NOD mice (n=6-7 mice/group, 105-116 islet/group) were assessed for immune cell infiltration. The insulitis was scored by the percentage of infiltration in each observed islet. Chi-square test was used for statistical analysis.

Figure S2 – Representative gating strategy of flow cytometry. **A**: Immune cells from splenocytes were first gated according to the SSA and FSC. The gated immune cells were further gated on the live cells using Zombie Dye (BioLegend). Gated live cells (Zombie Dye negative) were then gated using isotype control antibody (rat IgG2b) plot. Isotype control antibody negative but B200^{+} cells were selected for further B cell subset analysis. **B:** Representative flow cytometry plots of gating CD21 and CD23 after gating on B cells (B220^{+}).

Figure S3- The absolute cell number of different B cell subsets in different lymphoid tissues. Immune cells were isolated from different lymphoid tissues of *TLR9*$^{fl/fl}$/CD19-Cre- and *TLR9*$^{fl/fl}$/CD19-Cre-+ NOD mice (females, 6-8 weeks). Absolute cell numbers of different B cell subsets were calculated as percentage of each subset in flow cytometric analysis (10^5) multiplied by the total cell numbers harvested from each tissue. Graphical summaries of the different B cell subsets are shown (A-E). Data were pooled from 2 independent experiments and assessed for significance using an unpaired, two-tailed Student's t Test.

Figure S4 – B cell-specific TLR9 deficiency altered the frequency of B cell subsets in different lymphoid tissues at different age

A and **B** show graphical summaries of B cells expressing CD21^{high}CD23^{low} and CD21^{high}CD23^{high} in 6-8-week-old female mice (*n*=7/group). **C** and **D** show graphical summaries of B cells expressing CD21^{high}CD23^{low} and CD21^{high}CD23^{high} in 30-32-week-old non-diabetic female mice (*n*=4/group). Data were pooled from 2 independent experiments and assessed for significance using a Student's t test.

Figure S5- The differences in IgM^+ and IgD^+ single and double positive B cell subsets in different lymphoid tissues.

A-B demonstrate flow cytometric profiles from 6-8-week-old female mice (*n*=6/group); **A** shows a graphical summary of flow cytometric analysis of B cells expressing IgM^+IgD^-, while **B**, shows graphical summaries of the frequency of B cells expressing IgM^+IgD^+. Data were pooled from 2 independent experiments and assessed for significance using a Student's t test.

Figure S6- B cell-specific TLR9 deficiency decreased circulating IgG1.

Circulating immunoglobulins (IgM, IgA, IgG and IgG1) were assessed from the serum samples of 10-12-week-old female mice (n=4-8/group) by ELISA. The concentration of each isotype was calculated based on the standard curve, respectively. Two-tailed unpaired Student's t test was used for the statistical analysis.

Figure S7- B cell-specific TLR9 deficiency decreased $Blimp1^-$ plasmacytes. Immune cells from different lymphoid tissues were isolated from 6-8-week-old female mice (n=5/group) followed by staining with markers for B cells and plasmacytes and analysis by flow cytometry. **A**, proportion of B220+CD138-Blimp1+ plasmacytes; **B**, B220+CD138+Blimp1+ plasmacytes; **C**, B220+CD138+Blimp1- plasmacytes. Two-tailed unpaired Student's t test was used for the statistical analysis.

Figure S8- B cell-specific TLR9 deficiency did not affect CD8 T cells. Immune cells from different lymphoid tissues were isolated from 6-8-week-old female mice (n=5/group) followed by staining with the markers for different CD8+ T cells and analysis by flow cytometry. **A**, proportion of naïve CD8+ T cells (TCRβ+CD8+CD44-CD62L+); **B**, proportion of memory CD8+ T cells (TCRβ+CD8+CD44+CD62L-); **C**, proportion of IGRP-tetramer+ CD8 T cells (TCRVβ8+CD8+IGRP tetramer+). Two-tailed unpaired Student's t test was used for the statistical analysis.

Figure S89- B cell-specific TLR9 deficiency increased Treg cells. Immune cells from different lymphoid tissues were isolated from 6-8-week-old female mice (n=4-5/group) followed by staining with the Treg markers (TCRβ, CD4, CD25 and Foxp3). Two-tailed unpaired Student's t test was used for the statistical analysis.

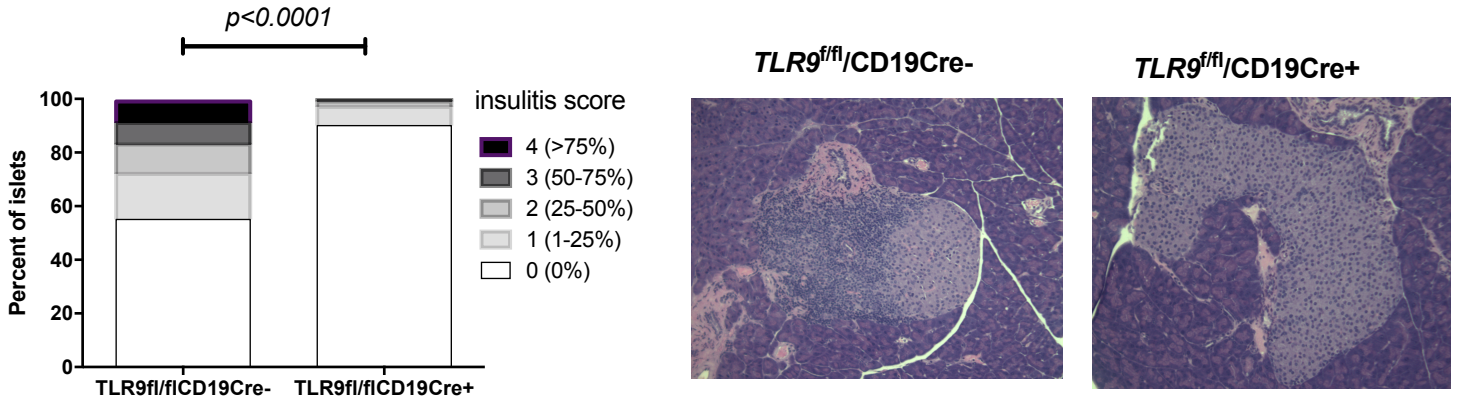
p<0.0001
Percent of islets
100
80
60
40
20
0
TLR9fl/flCD19Cre-
TLR9fl/flCD19Cre+
insulitis score
4 (>75%)
3 (50-75%)
2 (25-50%)
1 (1-25%)
0 (0%)
TLR9f/fl/CD19Cre-
TLR9f/fl/CD19Cre+

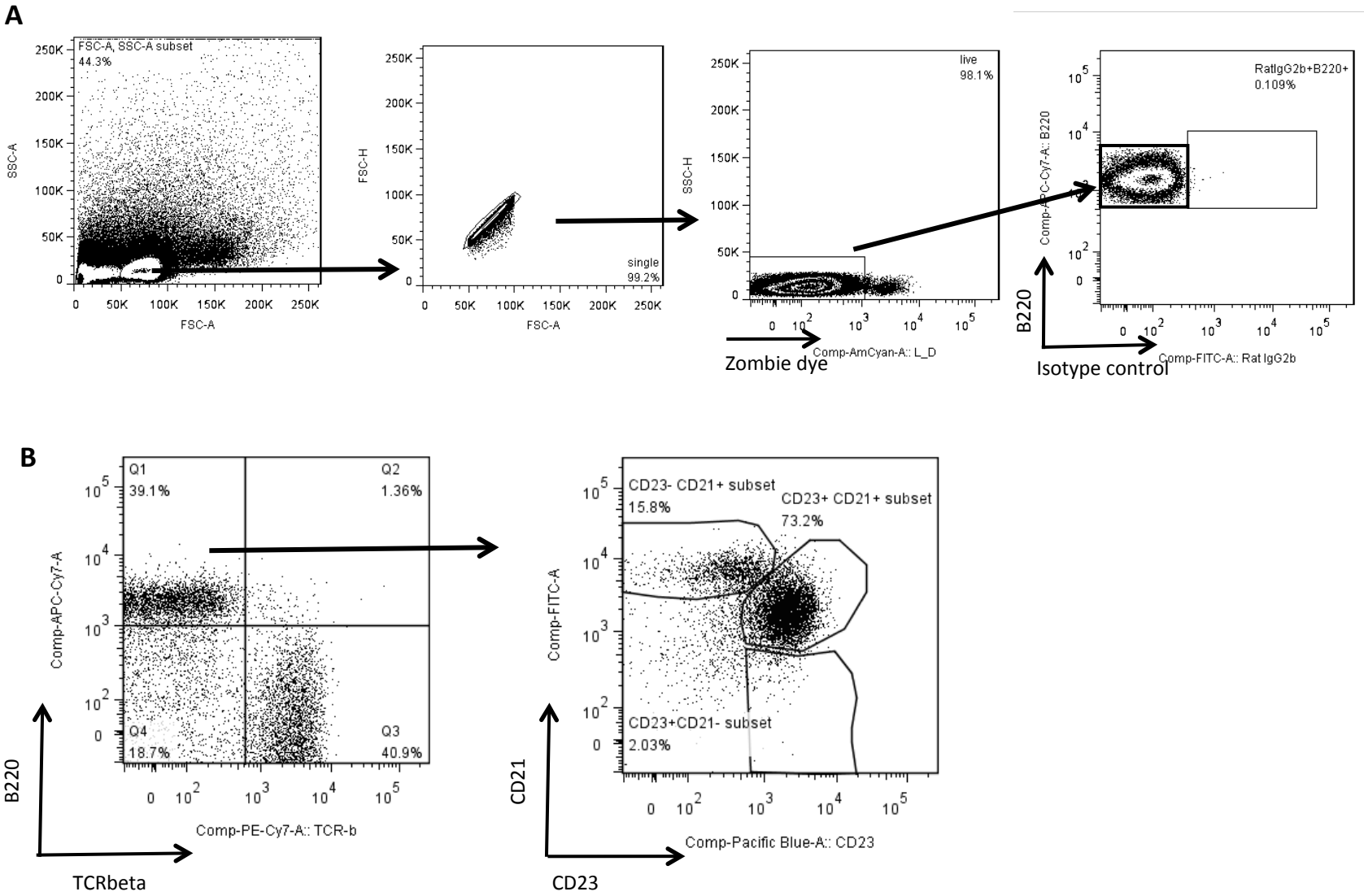
A
FSC-A, SSC-A subset
44.3%
SSC-A
FSC-A
FSC-H
single
99.2%
SSC-H
live
98.1%
Zombie dye
Comp-AmCyan-A:: L_D
RatIgG2b+B220+
0.109%
Comp-APC-Cy7-A:: B220
B220
Isotype control
Comp-FITC-A:: Rat IgG2b
B
Q1
39.1%
Q2
1.36%
Q4
18.7%
Q3
40.9%
Comp-APC-Cy7-A
B220
Comp-PE-Cy7-A:: TCR-b
TCRbeta
CD23- CD21+ subset
15.8%
CD23+ CD21+ subset
73.2%
CD23+CD21- subset
2.03%
Comp-FITC-A
CD21
Comp-Pacific Blue-A:: CD23
CD23

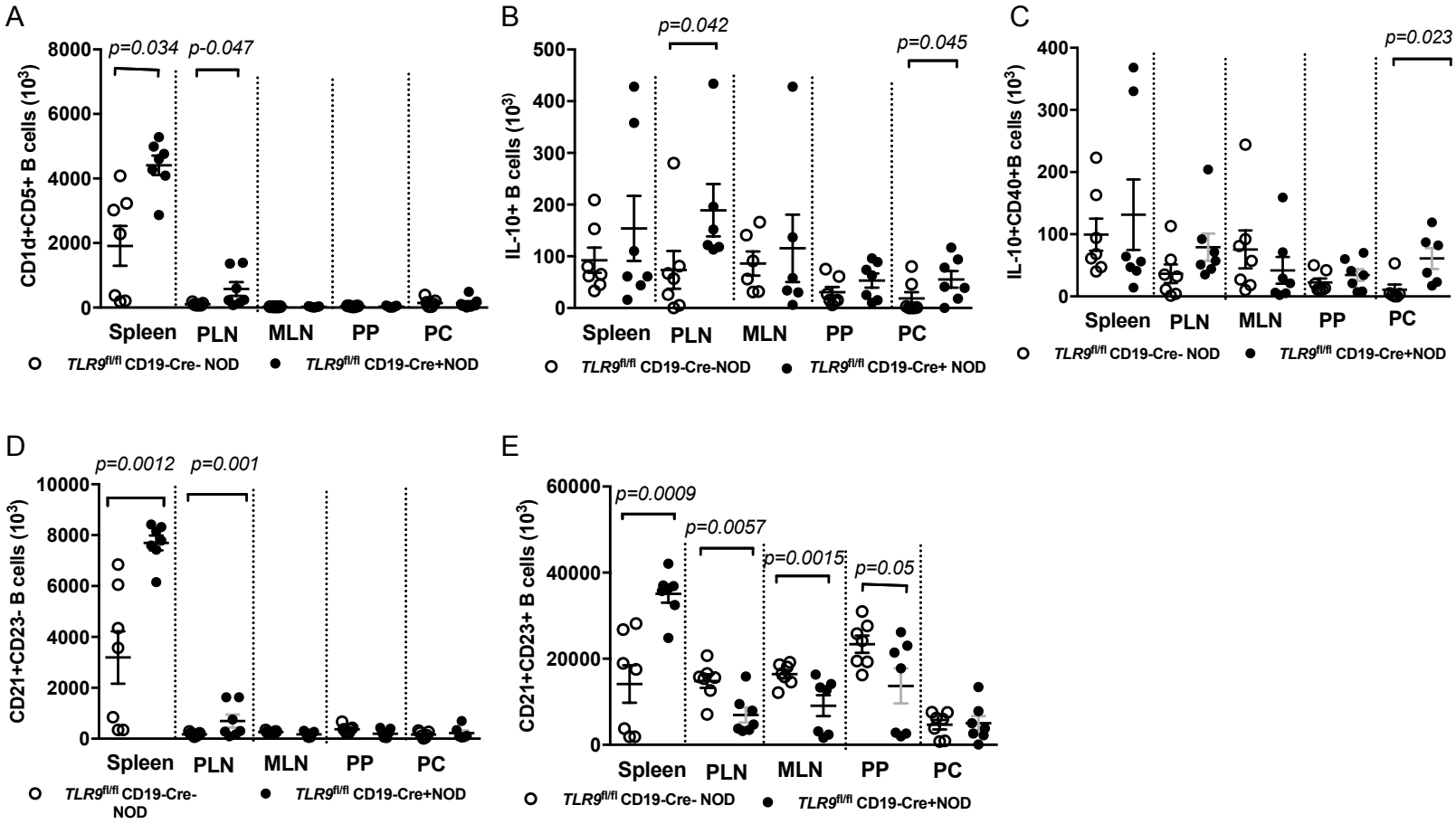
A
CD1d+CD5+ B cells (10^3)
p=0.034
p-0.047
Spleen
PLN
MLN
PP
PC
TLR9fl/fl CD19-Cre- NOD
TLR9fl/fl CD19-Cre+NOD
B
IL-10+ B cells (10^3)
p=0.042
p=0.045
TLR9fl/fl CD19-Cre-NOD
TLR9fl/fl CD19-Cre+ NOD
C
IL-10+CD40+B cells (10^3)
p=0.023
D
CD21+CD23- B cells (10^3)
p=0.0012
p=0.001
E
CD21+CD23+ B cells (10^3)
p=0.0009
p=0.0057
p=0.0015
p=0.05

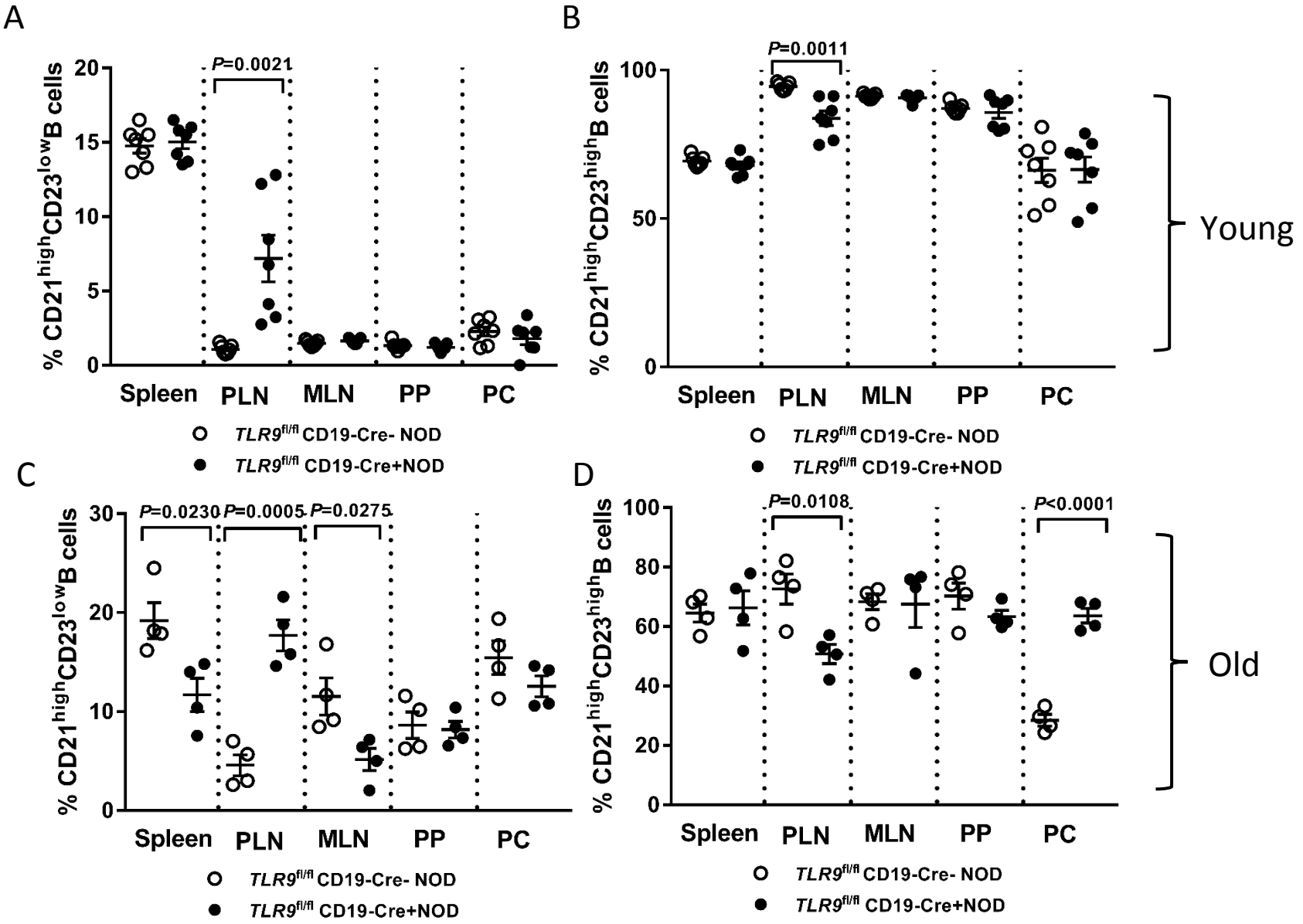
A
B
C
D
% CD21highCD23lowB cells
% CD21highCD23highB cells
P=0.0021
P=0.0011
P=0.0230
P=0.0005
P=0.0275
P=0.0108
P<0.0001
Spleen
PLN
MLN
PP
PC
TLR9fl/fl CD19-Cre- NOD
TLR9fl/fl CD19-Cre+NOD
Young
Old

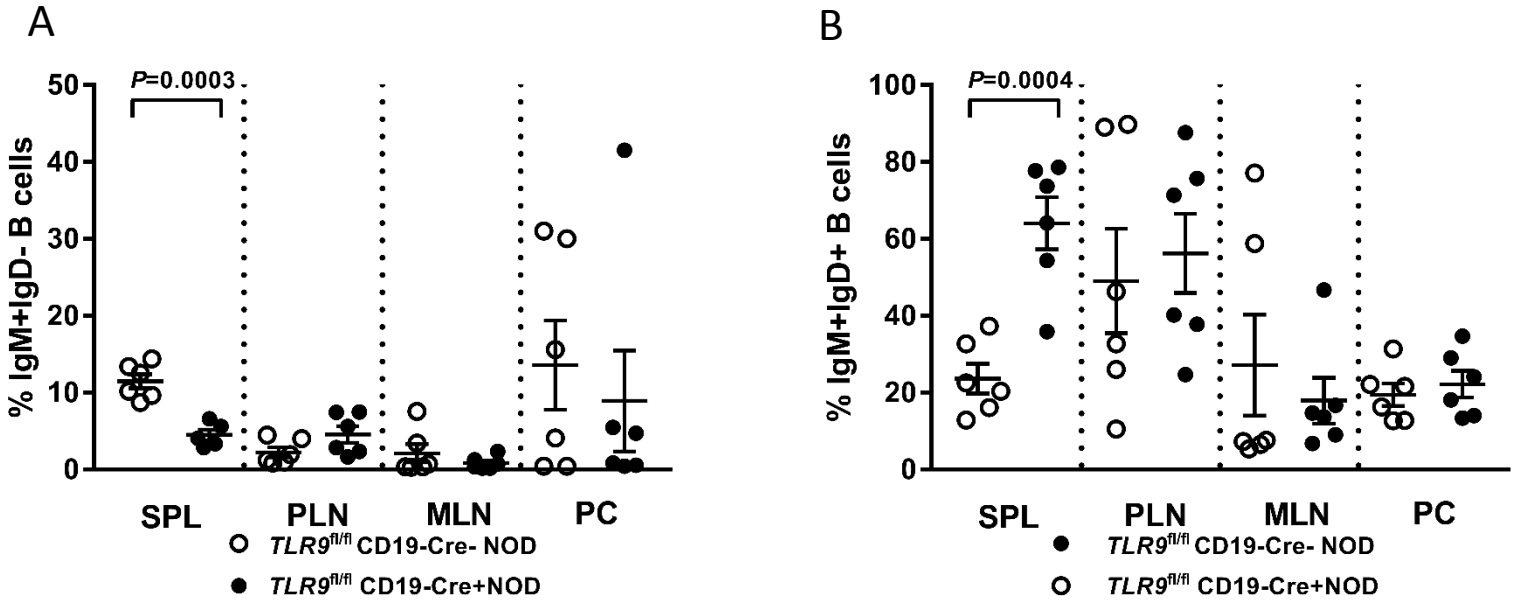
A
P=0.0003
% IgM+IgD- B cells
50
40
30
20
10
0
SPL
PLN
MLN
PC
TLR9fl/fl CD19-Cre- NOD
TLR9fl/fl CD19-Cre+NOD
B
P=0.0004
% IgM+IgD+ B cells
100
80
60
40
20
0
SPL
PLN
MLN
PC
TLR9fl/fl CD19-Cre- NOD
TLR9fl/fl CD19-Cre+NOD

Figure 5C

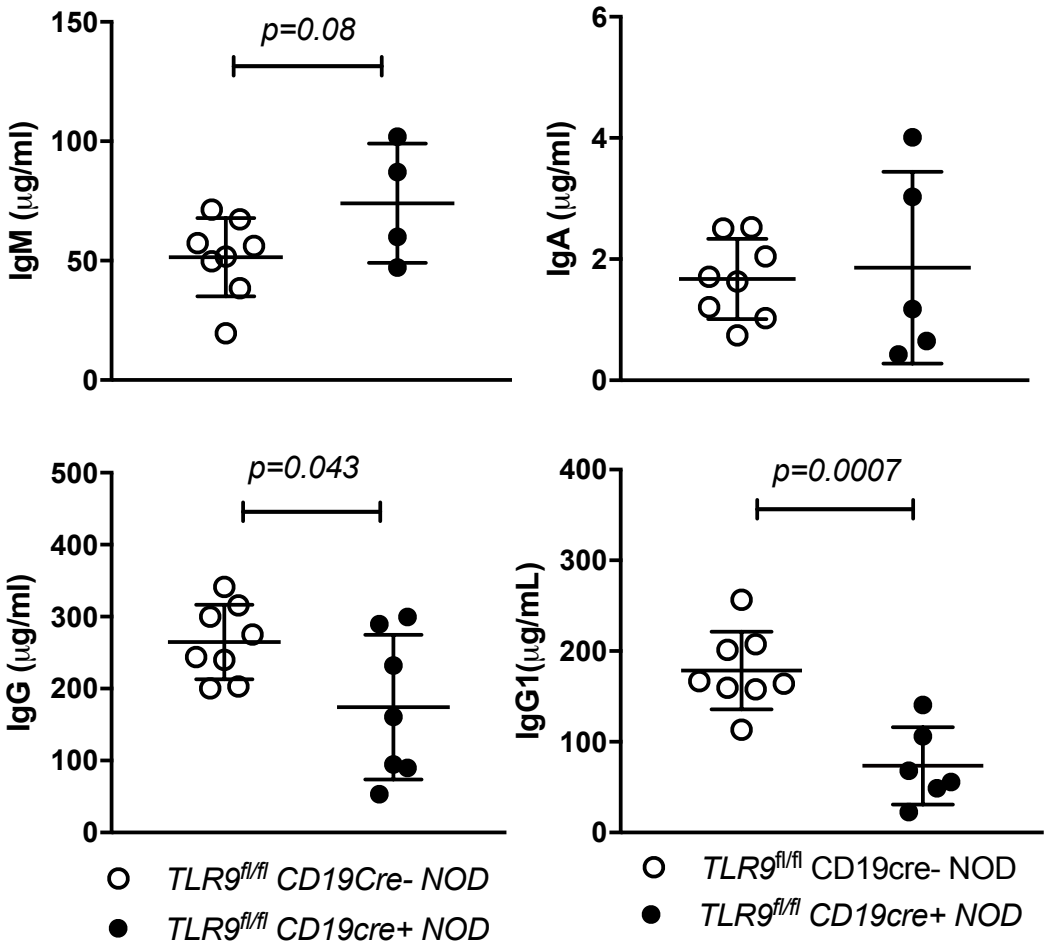
p=0.08
IgM (μg/ml)
150
100
50
0
IgA (μg/ml)
6
4
2
0
p=0.043
IgG (μg/ml)
500
400
300
200
100
0
p=0.0007
IgG1(μg/mL)
400
300
200
100
0
TLR9fl/fl CD19Cre- NOD
TLR9fl/fl CD19cre+ NOD
TLR9fl/fl CD19cre- NOD
TLR9fl/fl CD19cre+ NOD

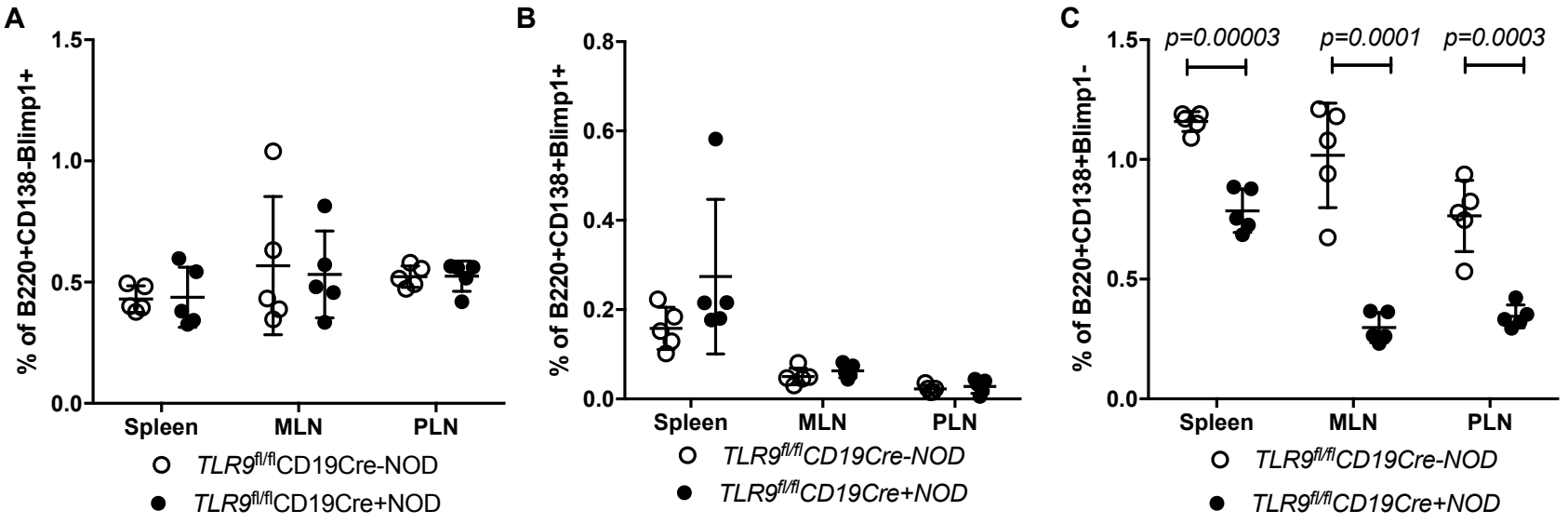
A
% of B220+CD138-Blimp1+
1.5
1.0
0.5
0.0
Spleen
MLN
PLN
TLR9fl/flCD19Cre-NOD
TLR9fl/flCD19Cre+NOD
B
% of B220+CD138+Blimp1+
0.8
0.6
0.4
0.2
0.0
Spleen
MLN
PLN
TLR9fl/flCD19Cre-NOD
TLR9fl/flCD19Cre+NOD
C
% of B220+CD138+Blimp1-
p=0.00003
p=0.0001
p=0.0003
1.5
1.0
0.5
0.0
Spleen
MLN
PLN
TLR9fl/flCD19Cre-NOD
TLR9fl/flCD19Cre+NOD

Figure 3B

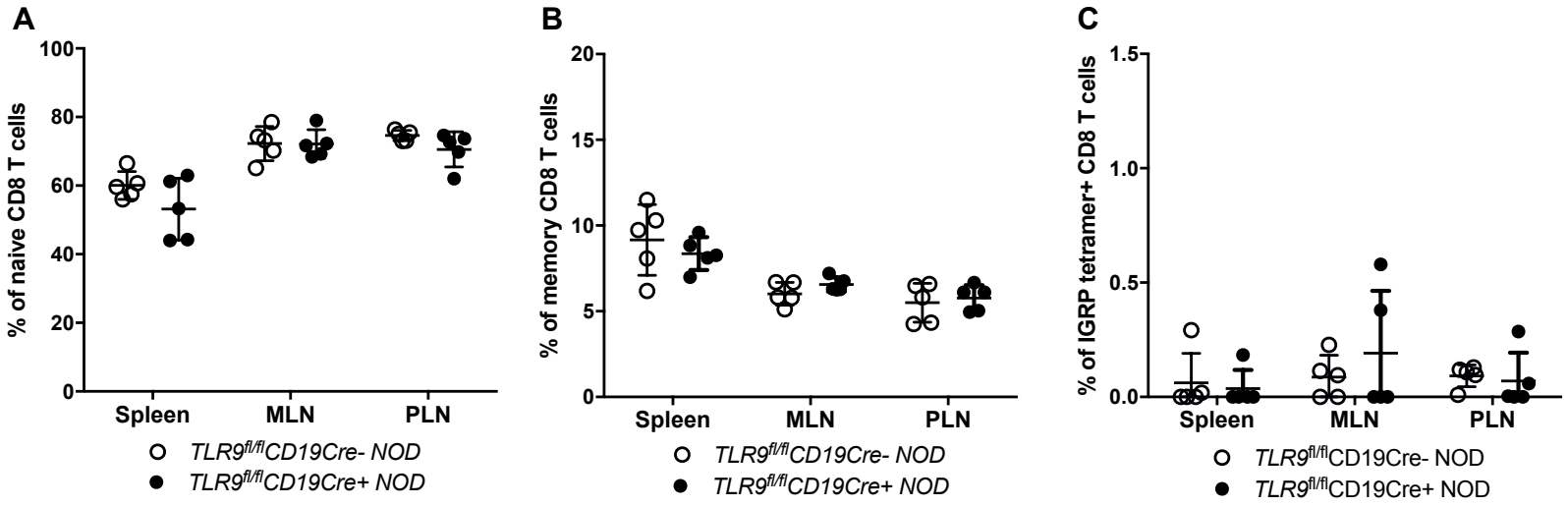
A
% of naive CD8 T cells
100
80
60
40
20
0
Spleen
MLN
PLN
TLR9fl/flCD19Cre- NOD
TLR9fl/flCD19Cre+ NOD
B
% of memory CD8 T cells
20
15
10
5
0
Spleen
MLN
PLN
TLR9fl/flCD19Cre- NOD
TLR9fl/flCD19Cre+ NOD
C
% of IGRP tetramer+ CD8 T cells
1.5
1.0
0.5
0.0
Spleen
MLN
PLN
TLR9fl/flCD19Cre- NOD
TLR9fl/flCD19Cre+ NOD

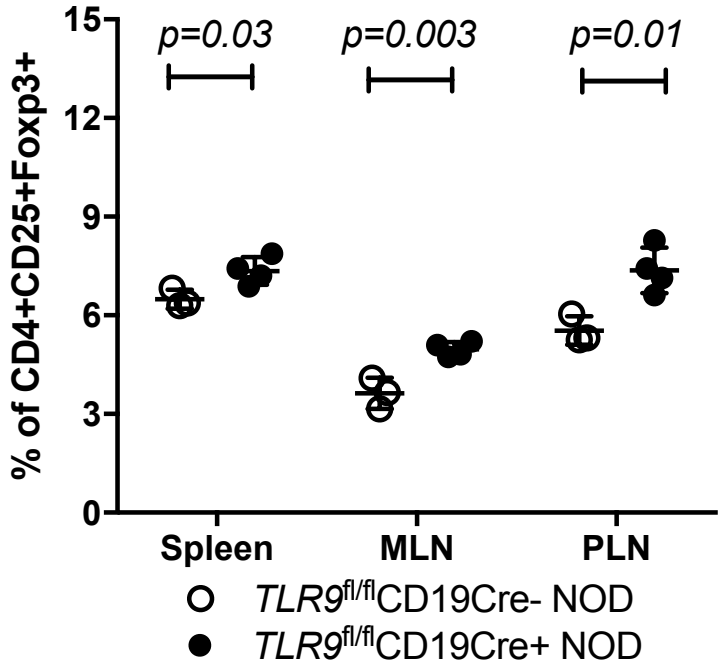
15
12
9
6
3
0
% of CD4+CD25+Foxp3+
p=0.03
p=0.003
p=0.01
Spleen
MLN
PLN
TLR9fl/flCD19Cre- NOD
TLR9fl/flCD19Cre+ NOD